AD_____

Award Number: W81XWH-10-1-0669

TITLE: UV-Induced Triggering of a Biomechanical Initiation Switch Within Collagen Promotes Development of a Melanoma-Permissive Microenvironment in the Skin

PRINCIPAL INVESTIGATOR: Peter Brooks, Ph.D.

CONTRACTING ORGANIZATION: Maine Medical Center
Portland, ME 04102-3134

REPORT DATE: November 2014

TYPE OF REPORT: Final

PREPARED FOR: U.S. Army Medical Research and Materiel Command
Fort Detrick, Maryland 21702-5012

REPORT DOCUMENTATION PAGE

Form Approved
OMB No. 0704-0188

1. REPORT DATE	2. REPORT TYPE	3. DATES COVERED
November 2014	Final	1Sep2010 - 31Aug2014

4. TITLE AND SUBTITLE
UV-Induced Triggering of a Biomechanical Initiation Switch Within Collagen Promotes Development of a Melanoma-Permissive Microenvironment in the Skin

5a. CONTRACT NUMBER

5b. GRANT NUMBER
W81XWH-10-1-0669

5c. PROGRAM ELEMENT NUMBER

6. AUTHOR(S)
Peter Brooks, PhD

E-Mail: brookp1@mmc.org

5d. PROJECT NUMBER

5e. TASK NUMBER

5f. WORK UNIT NUMBER

7. PERFORMING ORGANIZATION NAME(S) AND ADDRESS(ES)

Maine Medical Center
22 Bramhall Street
Portland, ME 04102-3134

8. PERFORMING ORGANIZATION REPORT NUMBER

9. SPONSORING / MONITORING AGENCY NAME(S) AND ADDRESS(ES)

U.S. Army Medical Research and Materiel Command
Fort Detrick, Maryland 21702-5012

10. SPONSOR/MONITOR'S ACRONYM(S)

11. SPONSOR/MONITOR'S REPORT NUMBER(S)

12. DISTRIBUTION / AVAILABILITY STATEMENT

Approved for Public Release; Distribution Unlimited

13. SUPPLEMENTARY NOTES

14. ABSTRACT The overall objective of our proposal was to test whether UV irradiation facilitates the exposure of the HU177 cryptic epitopes which may represent a "solid state biomechanical initiation switch" that promotes inflammation, skin damage and the creation of a melanoma permissive niche. We have successfully completed the majority of the experiments outlined in our original proposal. Overall, our studies indicate that the UV-irradiation of triple helical collagen in vitro, in the absence of proteolytic enzymes can induced changes in the structure of collagen that results in the exposure of the HU177 cryptic collagen epitope. UV-mediated triggering of the "HU177 biomechanical collagen switch" depended on the precise dose and wavebands of UV irradiation used and the type and preparation of ECM proteins evaluated. Importantly, UV-irradiation of full thickness skin resulted in exposure of the HU177 epitope, which was associated with elevated levels of inflammatory infiltrates including neutrophils, macrophages and mast cells. Pre-treatment of mice with anti-HU177 epitope antibody inhibited UV-induced mast cell accumulation and decreased UV-induced melanoma tumor growth in vivo. These data are consistent with the ability of UV-irradiation induced exposure of the HU177 cryptic collagen epitope in creating an inflammatory and tumor permissive microenvironment in the skin. Taken together, our data are consistent with the possibility that strategies might be developed that could selectively target the HU177 collagen epitope and be used prior to long term sun exposure to limit inflammation, and skin damage resulting from solar irradiation.

15. SUBJECT TERMS
Biomechanical switch -- Collagen structure -- Conformational change -- Cell adhesion -- Melanoma cells – Fibroblast-- Macrophages

16. SECURITY CLASSIFICATION OF:			17. LIMITATION OF ABSTRACT	18. NUMBER OF PAGES	19a. NAME OF RESPONSIBLE PERSON
a. REPORT	b. ABSTRACT	c. THIS PAGE			USAMRMC
Unclassified	Unclassified	Unclassified	UU	34	19b. TELEPHONE NUMBER *(include area code)*

Table of Contents

1. Introduction: The overall objective of our project was to test whether UV irradiation facilitates the exposure of the HU177 cryptic collagen epitopes which may represent a "solid state biomechanical initiation switch" that promotes inflammation, skin damage and the creation of a melanoma permissive niche. In particular, we proposed to examine whether targeting the HU177 biomechanical initiation switch prevents or reduces UV-induced inflammation and determine whether targeting these cryptic collagen sites (1-4) represent a useful approach to prevent and/or reduce melanoma growth. We have characterize the kinetics of UV-induced exposure of the HU177 cryptic epitopes in vitro and in vivo using a combination of biochemical assays, ELISAs and immunohistochemical analysis of UV irradiated-collagen as well as the basement membrane preparation Matrigel™. In the second aim, we evaluated the impact of UV-induced alterations in collagen and the basement membrane preparation Matrigel™ on inflammatory cell, dermal fibroblast, and melanoma cell adhesion, migration, invasion and proliferation as compared to controls. Finally, we examined the biological consequences of UV-induced exposure of the HU177 cryptic epitope on inflammatory cell infiltration and on the ability of melanoma cells to establish tumors in vivo.

2. Key Words:
1). Melanoma
2). Collagen
3). Tumor Growth
4). Inflammation
5). UV-Irradiation
6). Mast Cells
7). Macrophages
8). Fibroblasts
9). Angiogenesis
10). Cell Migration
11). Cell adhesion.
12). Cell Proliferation
13) Extracellular Matrix
14). Matrigel™
15). Cryptic Epitopes

3. Overall Project Summary: The overall objective of this proposal was to test the central hypothesis that UV irradiation facilitates the acute exposure of the HU177 cryptic collagen epitope which may represent an early solid state biomechanical initiation switch that promotes inflammation, skin damage and the creation of a melanoma permissive niched. To address this hypothesis we proposed 3 aims. In the first aim, we characterized the kinetics of UV-induced exposure of the HU177 cryptic epitopes in vitro and in vivo using a combination of biochemical assays, ELISAs and immunohistochemical analysis of UV irradiated-collagen as well as the basement membrane preparation Matrigel™. In the second aim, we assessed the impact of UV-induced alterations in collagen and the basement membrane preparation Matrigel™ had on inflammatory cell, dermal fibroblast, and melanoma cell adhesion, migration, invasion and proliferation as compared to control. Finally, in the third aim we examined the biological consequences of UV-induced exposure of the HU177 cryptic epitope on inflammatory cell infiltration and on the ability of melanoma cells to establish tumors in vivo. The overall summary of the experimental findings for each of the aims as they relate to the particular tasks outlined in the statement of work is provided below.

Aim-1 Summary: In task 1 of aim 1 we analyzed UV-mediated exposure of the HU177 cryptic collagen epitope within collagen type-I, type-IV and in the basement membrane preparation Matrigel™. As detailed in our previous progress reports (Appendix Figs 1,2,10, 27) and in the new data presented below, the ability of UV irradiation to expose the HU177 cryptic collagen epitope within isotype specific forms of collagen or Matrigel™ was determined to be waveband (UVA365 and UVB310) and dose dependent. Specifically, our

data suggest that irradiation of collagen type-I with UVA minimally enhanced the exposure the HU177 cryptic epitope and co-incubation with the reactive oxygen species (ROS) scavenger SOD had little impact on exposure of the HU177 epitope (figure 1A-C). Enhancement of the HU177 epitope was also observed in collagen type-IV (Appendix Fig 2). Interestingly, UVA (365nm) irradiation decreased expression of the HU177 epitope in Matrigel™ and co-incubation with the SOD had little effect (figure 1D-F).

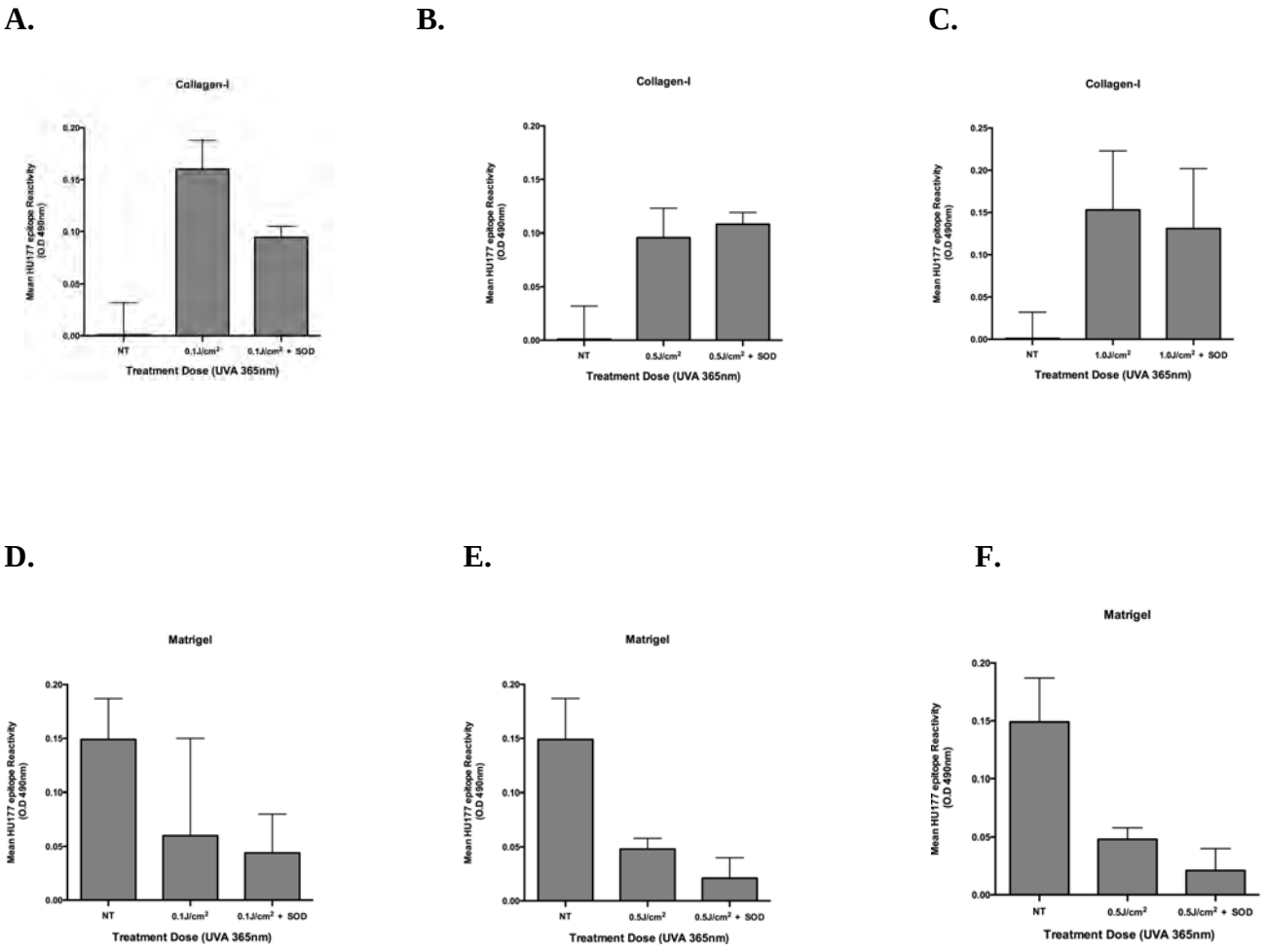

Figure 1. UVB-irradiation of collagen type-I and Matrigel™ differentially impacts exposure of the HU177 cryptic epitope. Collagen type-I or Matrigel™ was either not treated (NT) or irradiated with UVA (365nm) (0-1.0J/cm^2) in the presence or absence of SOD (25U/ml). Wells were coated and solid phase ELISAs was carried out to assess exposure of the HU177 epitope with Mab D93. (A-C) Reactivity of HU177 epitope in collagen-I. (D-F) Reactivity of HU177 epitope in Matrigel™. Data bars represent mean reactivity (Optical Density O.D) $\pm$ standard deviations.

In a similar set of studies, ECM proteins were irradiated with UVB (310nm) and this caused a dose dependent exposure of the HU17 epitope in collagen type-I, and type-IV, however inconsistent changes were observed within Matrigel™ (Appendix Figs 10 and 27). As shown in figure 2 A-C, UVB induce enhanced exposure of the HU177 epitope in both collagen –I and IV and this enhanced exposure was reduced by co-incubation with SOD, suggesting a role for ROS in this process. As mentioned above, inconsistent exposure of the HU177 epitope was observed following UVB irradiation of Matrigel™ and SOD had little effect. These data suggest that distinct wavebands of UV-irradiation can differential effect the three-dimensional structure of collagen, which was at least partially dependent on generation of ROS.

A. **B.** **C.**

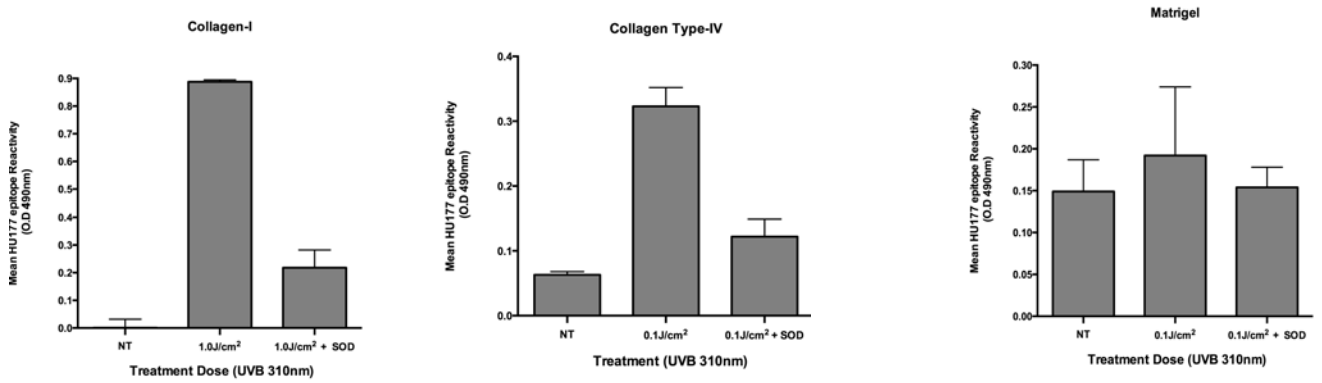

Figure 2. UVB-irradiation of collagen type-I, IV and Matrigel™ differentially impacts exposure of the HU177 cryptic epitope. Collagen type-I, IV or Matrigel™ was either not treated (NT) or irradiated with UVB (310nm) (0.1J/cm^2) in the presence or absence of SOD (25U/ml). Wells were coated and solid phase ELISAs was carried out to assess exposure of the HU177 epitope with Mab D93. (A) Reactivity of HU177 epitope in collagen-I. (B) Reactivity of HU177 epitope in collagen-IV. (C) Reactivity of HU177 epitope in Matrigel™ . Data bars represent mean reactivity (Optical Density O.D) $\pm$ standard deviations.

In task 2 of aim 1, we analyzed the exposure of the HU177 epitope within full thickness skin. As detailed in progress report 2 (Appendix Fig 24) while some low level expression of the HU177 epitope was detected in explanted human skin under non-UV-irradiated conditions confined largely to the lower region of the dermis, enhanced levels of the HU177 epitope was detected following UVB –irradiation at a dose of 1.0J/cm^2. In addition, as shown in figure 3 below, enhanced exposure of the HU177 epitope was also detected in murine skin following UVB-irradiation. Again, low level of expression of the HU177 was detectable in the lower region of the dermis in non-irradiated skin. Collectively, these data indicate that the HU177 cryptic collagen epitope can be induced within full thickness skin following UV-irradiation and that the distribution of the epitope appears to be predominately expressed within basement membrane structures.

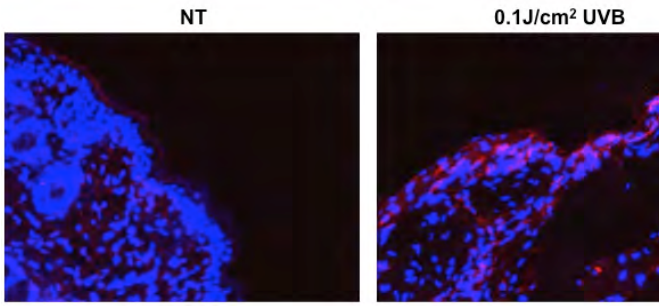

Figure 3. Elevated levels of the HU177 epitope detected in UVB-irradiated skin. Murine skin from non-treated (NT) or UVB irradiated (0.1J/cm^2) animals were stained for expression of the HU177 epitope with anti-HU177 antibody Mab D93 (Red). Dapi stain indicated in blue.

In task 3 of aim 1, we analyzed the expression of proteolytic enzymes within full thickness skin following UV irradiation (Appendix Fig 21). In addition, we also assessed the infiltration of stromal cells and immune cells. As detailed previously (Appendix Figs 18-20), we observed a dose and time dependent increase of inflammatory infiltrates within the dermal region of the skin. Importantly, at low doses of UVB and at early time points following irradiation (24hrs), the inflammatory infiltrates were largely confined to the subcutaneous fat with minor infiltration into the lower regions of the dermis. At high dose and following a longer time course (48-72hrs) enhanced infiltration into the upper regions of the dermis was observed (appendix Figs 18-10). In further studies, we analyzed neutrophil infiltration using the well-characterized marker A/4 antigen. As expected, relatively few neutrophils were detected in non-irradiated skin. In contrast, 24hrs following irradiation, a dose dependent enhancement of neutrophil infiltration was observed (Appendix Fig 19-22). Moreover, 48 hours following irradiation a dose dependent enhancement of macrophage infiltration was also observed (Appendix Fig 22). Interestingly, following UVB –irradiation of skin, a redistribution of αSMA expressing activated fibroblast-like cells were observed within the lower region of the dermis that was not readily apparent in the skin of non-irradiated mice (Appendix Fig 25). These data are consistent with the possibility that UV-irradiation results in altered αSMA expressing fibroblast migration. Given the enhanced infiltration of inflammatory cells including neutrophils and macrophages along with altered localization of αSMA expressing activated fibroblast, we examined the expression of proteolytic enzymes. As detailed in progress report 2, enhanced expression of neutrophil elastase as well as elevated levels of MMP-9 were readily detected following UV-irradiation (Appendix Fig 21). Taken together, while we provided evidence that UV-irradiation of purified collagen in vitro in the absence of proteolytic enzymes can results in structural changes leading to the exposure of the HU17 epitope, the enhanced presence of proteolytic enzymes following UV-irradiation in vivo likely contributes to elevated expression of the HU177 cryptic collagen epitope within full thickness skin.

Aim-2 Summary: In task 1 of aim 2, we analyzed the impact of UV-induced exposure of the HU177 epitope on cell adhesion. As detailed in our previous progress reports 1 through 3, cell type and ECM specific alterations in cell adhesion were observed following UV-irradiation of ECM proteins (Appendix Figs 3-7, 11,12,29,30,32). In particular, melanoma cell (M21) adhesion to both UVA and UVB irradiated collagen type-I and IV were dose dependently enhanced as compared to non-irradiated collagen. Interestingly, while enhanced M21 melanoma cell adhesion was observed on UVA-irradiated Matrigel^{TM}, a dose dependent decrease in M21 cell adhesion was observed UVB-irradiated Matrigel^{TM} . These interesting observations suggest that distinct wavebands of UV-irradiation alter the exposure of structural epitopes that are capable of mediating melanoma cell adhesion to the complex basement membrane preparation Matrigel^{TM}. Interestingly, fibroblast adhesion was enhanced on UVB-irradiated collagen type-I, collagen type-IV and Matrigel^{TM}. These findings are in good agreement with the enhanced re-localization of fibroblast-like cells to basement membranes observed in the lower regions of the dermis following UVB-irradiation of skin. Given the enhanced infiltration of inflammatory cells following UV-irradiation, we also examined the differential adhesive interactions of RAW macrophage cell line and a mast cell line (Appendix Figs 5 and 32). As was shown with melanoma cells and stromal fibroblasts, macrophage and mast cells exhibited differential adhesion to UV-irradiated proteins. Specifically, while little change in macrophage cell adhesion was observed following UVB-irradiation of collagen, a dramatic enhancement of macrophage adhesion to UVB-irradiated collagen-IV was observed, while mast cells showed little change in adhesive differences on non-irradiated or UVB irradiated collagen type-IV but enhanced adhesion to irradiated collagen type-I and Matrigel^{TM}.

In task 2 of aim 2, we analyzed the impact of UV-induced exposure of the HU177 epitope on cell migration. As expected, similar to the experimental findings observed with cell adhesion, alterations of cell migration were UV-dose dependent and cell type and ECM specific (Appendix Figs 14,16,26,32). As detailed in previous progress reports, while enhanced migration was observed with M21 melanoma cell on UV-irradiated Matrigel^{TM}, migration of Raw macrophages was dose dependently inhibited (Appendix Figs 14 and 16). In contrast, minimal changes in fibroblast migration were observed following low dose UV-irradiation of Matrigel^{TM} , however, at higher doses of UVB, reduced cell migration was observed (figure 4D). Interestingly,

Mab D93 directed to the HU177 epitope had little impact on fibroblast migration on irradiated ECM substrates (fig 4 A-D).

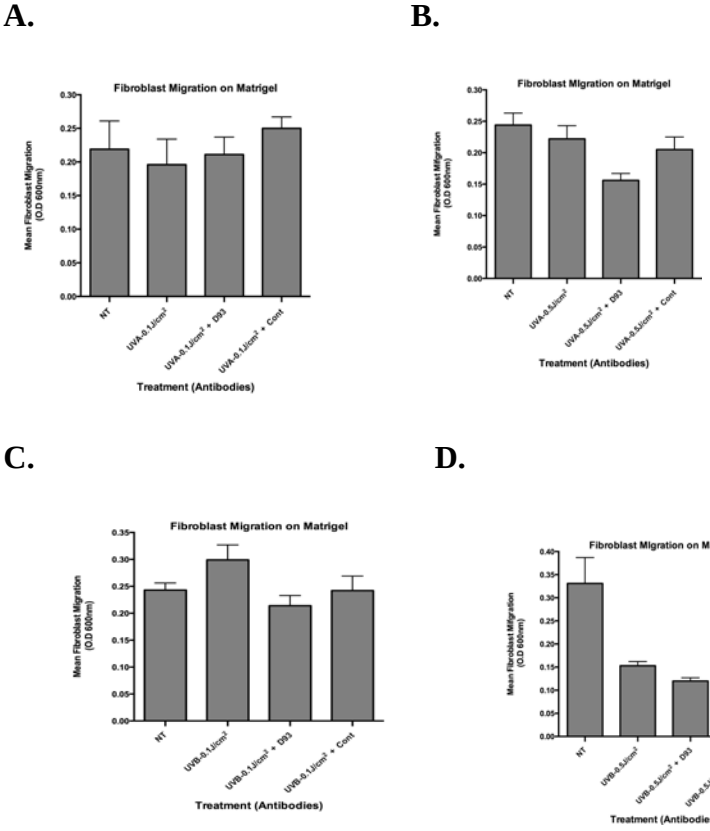

Figure 4. Differential impact of UVB irradiation on migration of dermal fibroblasts on Matrigel™. Matrigel™ was either non-treated (NT) or irradiated with UVA (365nm) or UVB (310nm) over a dose range (0-0.5J/cm^2). Matrigel™ was coated on membranes from transwell inserts and blocked with BSA. Human dermal fibroblasts were seeded on the wells and allowed to migrate. Data bars represent mean cell migration (Optical Density O.D) ± standard deviations from triplicate wells.

In task 3 of aim 2, we analyzed the impact of UV-induced exposure of the HU177 epitope on cell proliferation (Appendix Figs 8,9,13,15,17). As detailed in our previous progress report 2, while little change in M21 cell proliferation was observed on UVB-irradiated Matrigel™, enhanced macrophage proliferation was seen. Interestingly, while enhanced fibroblast proliferation was observed on UVA-irradiated Matrigel™ little change in proliferation was observed on UVB-irradiated Matrigel™ over a dose range (figure 5A-C). Incubation with SOD had little effect on fibroblast growth on either non-irradiated or UV-irradiated Matrigel™.

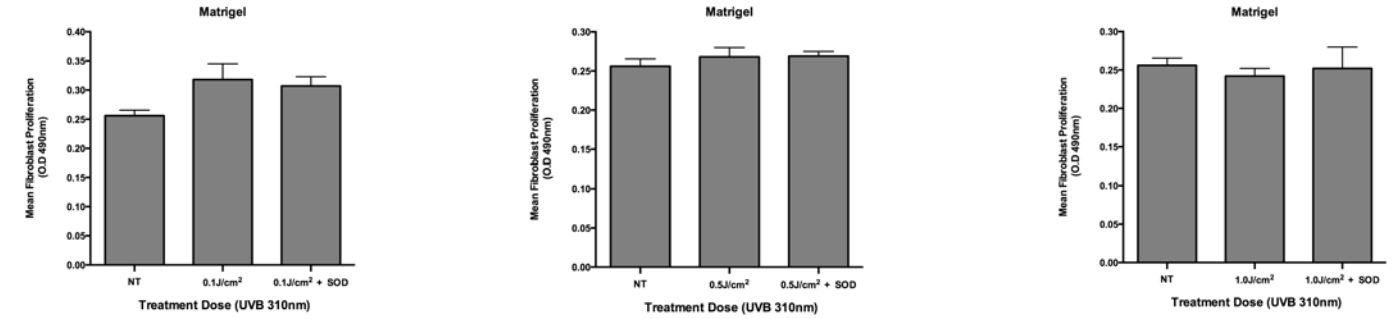

Figure 5. Effects UVB-irradiation of Matrigel™ on fibroblast proliferation. Matrigel™ was either not treated (NT) or irradiated with UVB (310nm) at a dose (0 to 1.0J/cm^2) in the presence or absence of SOD and wells were coated. Human dermal fibroblasts were resuspended in buffer and added to the wells. Proliferation was quantified by MTT assays. A) Fibroblast proliferation on 0.1J/cm^2 irradiated Matrigel™. B) Fibroblast proliferation on 0.5J/cm^2 irradiated Matrigel™. C) Fibroblast proliferation on 1.0J/cm^2 irradiated Matrigel™. Data bars represent mean cell proliferation (Optical Density O.D) ± standard deviations from triplicate wells.

Taken together, while a clear increase in fibroblast proliferation on UVA (365)-irradiated Matrigel™ was observed, minimal if any effects were seen on collagen I or IV following UVB irradiation again indicating a specific effect of distinct wavebands of UV-irradiation on ECM dependent cell proliferation.

Aim-3 Summary: In task 1 of aim 3, we analyzed the impact of UV-induced exposure of the HU177 epitope on inflammatory cell and stromal cell infiltration of full thickness skin and on the ability melanoma cells to establish tumors in vivo. As detailed in our previous progress report 2, UVB-irradiation of full thickness skin was associated with a dose dependent and time dependent infiltration of multiple inflammatory infiltrates including neutrophils and macrophages as well as a re-localization of activated fibroblast-like cells (Appendix Figs 18-25, 33,34). Interestingly, further studies indicated an increase in infiltration and accumulation of mast cells within the upper region of the dermis and epidermal compartments (Appendix Figs 18,21,22). Given that mast cells are known to be among some of the earliest inflammatory infiltrates to appear following irradiation, we examined the effects of pre-treating mice with antibody Mab D93 specifically directed to the HU177 cryptic collagen epitope. As discussed previously in progress report 2, pre-treatment with Mab D93 but not control antibody, inhibited the enhanced mast cell accumulation following UVB-irradiation (Appendix Fig 22). To confirm these results, similar experiments were performed. As shown in figure 6A below, a low dose of UVB irradiation (0.1J/cm^2) applied to the skin of nude mice resulted in inflammation as indicated by enhanced reddening of the skin and dilation and of the associated vasculature. Interestingly, a single (i.p) pre-treatment with Mab D93 of the mice prior to UV-irradiation dramatically reduced the UV-induced reddening and vessel dilation as compared to control. Moreover, quantification of mast cell infiltration following UV-irradiation showed a significant reduction to near base line levels in mice pre-treated with anti-HU177 Mab as compared to non-specific control antibody (figure 6B). These findings confirm our previous observation and suggest a functional role for the HU177 epitope in regulating UV-induced mast cell accumulation and inflammation in the skin.

A. **B.**

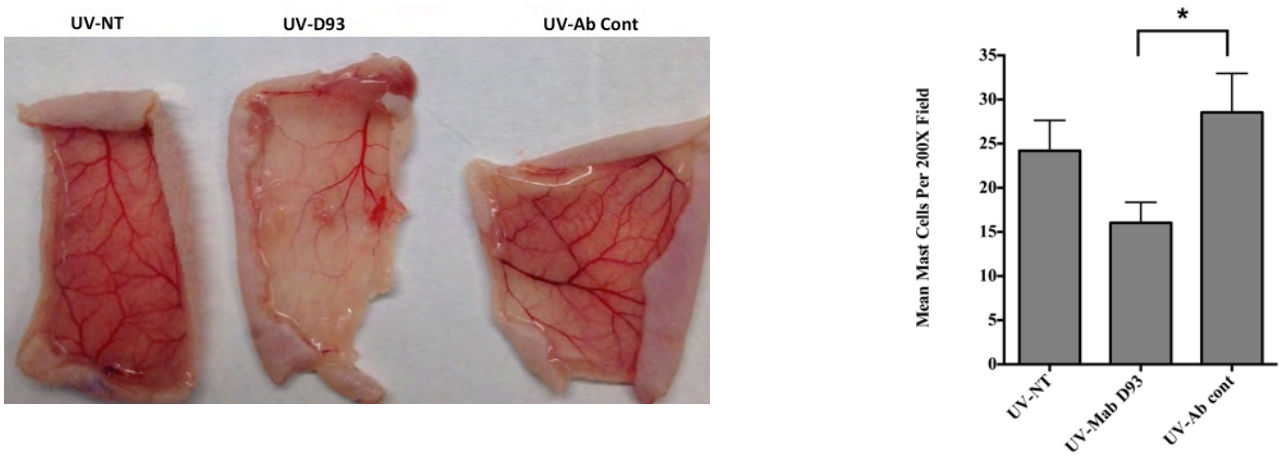

Figure 6. Pre-treatment of mice with anti-HU177 antibody reduced UVB-induced skin inflammation and mast cell accumulation. Nude mice were either not treated (NT) or pre-treated with a single i.p injection of Mab D93 (100ug/mouse). Twenty-four hours later, mice were either not treated or irradiated with UVB (310nm) at dose of 0.1J/cm^2. Twenty-four hour later mice were sacrificed and skin dissected and mast cells quantified. A) Representative example of mouse skin from each condition. B) Quantification of mast cell infiltration. Data bars represent mean mast cells per 200X field from 10 fields per mouse.

To study the role of the HU177 collagen epitope in UV-induced tumor growth in more detail, we examine the relative expression of the HU177 epitope within M21 melanoma tumors that formed from non-irradiated and

UVB-irradiated mice. As shown in figure 7A below, enhanced detection of the HU177 epitope was observed within tumors growing in UV-irradiated mouse skin as compared to control. Interestingly, the distribution of the HU177 epitope appeared consistent with a close association with vascular basement membranes. Given our previous studies suggest a distinct re-localization of activated fibroblast like cells into region of the UV-irradiated skin that were closely associated with basement membranes, these M21 melanoma tumors were co-stained for fibroblasts expressing fibroblast activation protein (FAP) and a well characterized marker of blood vessels CD-31 (5,6). As shown in figure 7B below, elevated levels of FAP-expressing -tumor associated fibroblasts were detected surrounding CD-31 positive blood vessels as compared to tumors growing in non-irradiated skin. These data are consistent with the possibility that UV-irradiation may stimulate recruitment of activated fibroblasts into close proximity of tumor-associated blood vessels.

A.

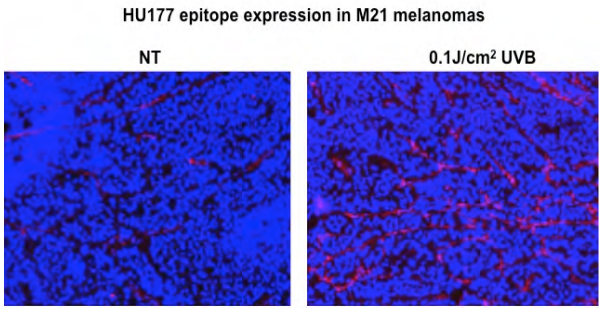

B.

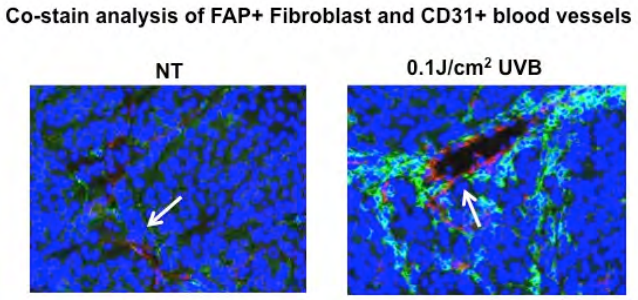

Figure 7. Enhances exposure of the HU177 cryptic collagen epitope in melanoma tumors growing in UVB-irradiated skin. Nude mice were either not treated (NT) or irradiated with UVB (310nm) at a dose of 0.1J/cm^2. Twenty-four hours latter mice were injected with M21 melanoma cells and tumors were allowed to grow for three weeks. A) Example of expression of the HU177 epitope (Red) as indicated by staining with Mab D93 in frozen section of tumor tissue from each condition. B). Example of co-distribution of FAP expressing cancer associated fibroblasts and CD-31 expressing blood vessels within frozen sections of tumor from each condition.

4). Key Research Accomplishments:

1). UVA and UVB specifically and differential triggers exposure of the HU177 cryptic collagen epitope in a dose dependent manner within collagen type-I, type-IV and the basement membrane preparation Matrigel^{TM}.

2). Reactive oxygen species (ROS) play only a modest role in the generation of the HU177 cryptic collagen epitope in vitro, which depends on the dose and wavebands of UV-irradiation used.

3). UV-irradiation can trigger the generation of the HU177 cryptic collagen epitope within full thickness human and mouse skin in vivo.

4). UV-irradiation associated generation of the HU177 cryptic collagen epitope was associated with a time and dose dependent increase infiltration of inflammatory neutrophils, mast cells and macrophages within full thickness skin.

5). The proteolytic enzymes neutrophil elastase and matrix metalloproteinase-9 were enhanced in full thickness skin following UV-irradiation.

6). UVA and UVB-irradiated collagen and Matrigel^{TM} in vitro differentially increased and/or decreased the adhesive behavior in a cell type specific manner.

7). UVA and UVB-irradiated collagen and Matrigel^{TM} in vitro differentially increased and/or decreased the migratory behavior in a cell type specific manner.

8). UVA and UVB-irradiated collagen and Matrigel^{TM} in vitro differentially increased and/or decreased the proliferative behavior in a cell type specific manner.

9). UVB-irradiation of full thickness skin prior to tumor cell injection results in enhanced M21 melanoma cell growth.

10). UVB-induced increase in M21 melanoma tumor growth in vivo was inhibited by pre-treatment with function blocking antibody directed to the HU177 epitope.

11). UVB irradiation enhanced the accumulation of mast cells in the skin in a UV- dose dependent manner.

12). The UVB-induced accumulation of mast cells in the skin depends in part on the generation of the HU177 epitope as pretreatment of mice with anti- HU177 epitope antibody inhibited UV-induced mast cell accumulation in the skin.

13). UVB-irradiation of mouse skin causes re-localization of activated fibroblasts into the basement membrane rich dermal regions of the skin.

14). UVB-irradiation of mouse skin causes enhanced levels of the HU177 epitope within M21 melanoma tumors in vivo.

15). Pre-treatment of mice with function blocking Mab directed to the HU177 cryptic epitope reduced the levels of αSMA express tumor associated fibroblasts in melanoma tumors growing in irradiated skin.

5). Conclusions:

The overall objective of our project was to test whether UV irradiation facilitates the exposure of the HU177 cryptic collagen epitopes which may represent a “solid state biomechanical initiation switch” that promotes inflammation, skin damage and the creation of a melanoma permissive niche. We proposed to examine whether specific targeting of the HU177 biomechanical initiation switch prevents or reduces UV-induced inflammation and to determine whether targeting these cryptic collagen sites represent a useful approach to prevent and/or reduce melanoma growth. We have successfully completed a majority of the experiments outlined in our original proposal. Taken together, our studies indicate that the UV-irradiation of triple helical collagen in vitro, in the absence of proteolytic enzymes can induced changes in the structure of collagen that results in the exposure of the HU177 cryptic collagen epitope. Surprisingly, our studies indicate the UV-mediated triggering of the “HU177 biomechanical collagen switch” depended on the precise dose and wavebands of UV irradiation used and the type and preparation of ECM proteins evaluated. Given that the majority of the solar irradiation that actually reaches the earth is a combination of both UVA and UVB (7) and the surprising differential effects of UV-wavebands on exposing the HU177 epitope in vitro, the exact extent of contribution of each individual waveband of UV in solar-irradiation as it relates to the generation of the HU177 cryptic collagen epitope in humans will be difficult to establish from our experimental results. However, our studies are consistent with the ability of UV-irradiation of full thickness skin to cause specific exposure of the HU177 collagen epitope. Interestingly, while our studies did detect generation of the HU177

epitope in non-irradiated skin, much of this epitope was confined to the lower regions of the dermis, and following UV-irradiation, enhanced generation of the HU177 epitope was detected in the epidermal layers of the mouse skin. Moreover, the enhanced levels of HU177 epitope following UV-irradiation was also associated with elevated levels of inflammatory infiltrates including neutrophils, macrophages and mast cells and increased levels of proteolytic enzymes. Thus, while in vitro studies clearly indicate hat the HU177 epitope can be generated from non-proteolytic mechanisms, given the enhanced levels of inflammatory infiltrates and proteolytic enzymes released in vivo, it is likely that distinct proteolytic mechanisms also contribute to the generation of the HU177 epitope during exposure of full thickness skin to UV-irradiation in vivo.

Our studies indicate that a variety of cell types are rapidly recruited to the sites of UV-exposed skin and the HU177 cryptic collagen epitope can be readily generated within both the epidermal and dermal regions of the skin. In this regard, our data indicate a highly complex and differential adhesive, migratory and proliferative behavior of cells on UV-irradiated ECM proteins. These cellular behaviors were cell type specific and remarkably, depended on the particular waveband and dose of UV used under specific experimental. Given the combination of distinct wavebands present within solar radiation, along with the relative proportions of each waveband, a more extensive and detailed analysis of UV-irradiation that more closely mimics the specific composition of solar irradiation is needed. However, our experimental results suggest the generation of the HU177 epitope by differential exposure of UV-wavebands can dramatically alter the behavior of specific cell types known to contribute to inflammation and skin damage following exposure to unprotected skin.

Importantly, our in vivo studies suggest that exposure of skin to UV-irradiation can generate the HU177 collagen epitope and the growth of melanoma cells within this microenvironment was increased. Moreover pre-treatment with a function-blocking antibody specifically directed to the HU177 collagen epitope inhibited UV-enhanced tumor growth. Surprisingly, pretreatment of mice with anti-HU177 antibody also specifically reduced the overall levels of αSMA expressing tumor-associated fibroblast. Give that fibroblast are a major cellular source of both proteolytic enzymes and collagen (8-10) and have been shown to play functional roles in tumor progression, inflammation and fibrotic responses, our data is consistent with the possibility that the reduced tumor growth observed may be associated in part with a reduction in the levels of tumor associated fibroblasts. Finally, our results also suggested that pre-treatment of mice prior to UV-irradiation reduced skin inflammation and mast cell accumulation indicting a specific functional role for the HU177 collagen epitope in this physiological response to UV-irradiation. When taken together, our data from this study provided evidence consistent with the possibility that specific strategies might be developed that could selectively target the HU177 collagen epitope that could be administered prior to long term sun exposure to limit inflammation, and skin damage resulting from solar irradiation. Given the close association of inflammation and recruitment of cancer-associated fibroblasts in contributing to melanoma development and progression, limiting skin damage from solar radiation is of considerable importance. In this regard, do to the unique nature of military operations in the field, military personnel are often required to perform critical tasks in outdoor environments, in which they may be subjected to high levels of solar UV irradiation to unprotected areas of the body for extended periods of time. Our studies provide unique insight into the role of UV-irradiation in creating an inflammatory and tumor permissive microenvironment in the skin that depends in part on the generation of the HU177 cryptic collagen epitope.

6). Publications, Abstracts and Presentations: Nothing to report.

7). Inventions, Patents, and Licenses: Nothing to report.

8). Reportable outcomes: None

9). Other achievements: Nothing to report:

10). References:

1). Petitclerc, E., Stromblad, S., von Schalscha, T. L., Mitjans, F., Piulats, J., Montgomery, A. M., Cheresh, D. A., and Brooks, P. C. Integrin αvβ3 promotes M21 melanoma growth in human skin by regulating tumor cell survival. Cancer Res. 59: 2724-2730. 1999.

2). Cretu, A., Roth, M., Caunt, M., Akalu, A., Policarpio, D., Formenti, S., Gagne, P., Liebes, L., and Brooks, P.C. Inhibition of Angiogenesis by Disrupting Endothelial Cell Interactions with the Novel HU177 Cryptic Collagen Epitope. Clin. Cancer. Res.13: 3068-3078. 2007.

3). Pernasetti F, Nickel J, Clark D, Baeuerle PA, Van Epps D, Freimark B. Novel anti-denatured collagen humanized antibody D93 inhibits angiogenesis and tumor growth: an extracellular matrix-based therapeutic approach. Int. J Oncol. 29:1371-9. 2006.

4). Freimark B, Clark D, Pernasetti F, Nickel J, Myszka D, Baeuerle PA, Van Epps D. Targeting of humanized antibody D93 to sites of angiogenesis and tumor growth by binding to multiple epitopes on denatured collagens. Mol. Immunol. 44: 3741-50. 2007.

5). Madar S, Goldstein I, Rotter V. Cancer associated fibroblasts-more than meets the eye. Trends Mo. Med. 8:447-53. 2013.

6). Xu, J., Rodriguez, D., Petitclerc, E., Kim, J. J., Hangai, M., Moon, Y. S., Davis, G. E. and Brooks, P. C. Proteolytic exposure of a cryptic site within collagen-IV is required for angiogenesis and tumor growth. J. Cell Biol. 154: 1069-1079. 2001.

7). Maddodi N, Jayanthy A, Setaluri V. Shining light on skin pigmentation: the darker and righter side effects of UV radiation. Photochem. Photobiol. 88:1075-82. 2012.

8). Kharaishvili G, Simkova D, Bouchalova K, Gachechiladze M, Narsia N, Bouchal J. The role of cancer associated fibroblasts, solid stress and other microenvironmental factors in tumor progression and therapy resistance. Cancer Cell Int. 16: 14:41. 2014.

9). Yin M, Soikkeli J, Jahkola T, Virolainen S, Saksela O, Hölttä E. Am J Pathol. TGF-β signaling activated stromal fibrolasts, and cysteine cathepsin B and L drive the invasive growth of human melanoma cells. Am. J. Pathol. 181: 2202-16. 2012

10). Wäster P, Rosdahl I, Gilmore BF, Seifert O. Ultraviolet exposure of melanoma cells induce fibroblast activation protein-α in fibroblasts: implications for melanoma invasion. Int. J. Oncol. 39:193-202. 2011.

11). Appendices: Appendix includes a summary of all figures and discussion from each of the prior progress reports.

Appendix:

Figure 1. UV-mediated exposure of the HU177 cryptic epitope within collagen. To begin to assess whether specific UV wavebands my trigger exposure of unique functional epitopes within collagen, we began establishing the experimental conditions to assess the exposure of the HU177 cryptic collagen epitope by ELISA. Our previous studies suggested that UVA irradiation might induce structural changes in basement membrane collagen type-IV. In an initial set of experiments to establish whether UV irradiation could lead to the exposure of the HU177 collagen epitope, microtiter plates coated with either collagen type-I or type-IV and then irradiated with UVA using an Entela UVM-18EL series UV lamp with a maximum 8Watt output. To achieve doses of UVA above 0.6J/cm^2, long exposure times were necessary including some exposure times over 6-12hrs. Extensive experimental analysis indicated that the long exposure times needed to achieve the UV doses resulted in alterations in optical properties of the microtiter wells within which the assays were being conducted. This technical problem prevented us from carrying out further analysis using the UVM-18EL series lamp with immobilized collagen on microtiter plates.

To circumvent this technical issue, we obtained a new UV lamp irradiation system (Tyler Research UV-1) with more accurate and higher power stable UV energy output, which allows shorter exposure periods to achieve the dose range needed. First, we performed a series of experiments to assess the effects of UV irradiation on exposure of the HU177 cryptic epitope within collagen prepared in solution, followed by coating on microtiter plates. Following extensive optimization to insure sensitive detection of the epitope, we examined the exposure of the HU177 epitope within interstitial collagen type-I over a dose range (0.05J/cm^2-5.0J/cm^2) of UVB (310nm). As shown in figure 1, irradiation of collagen type-I in solution with doses of UVB at 5.0J/cm^2 resulted in exposure of the HU177 cryptic collagen epitope. While a small degree of exposure of the HU177 epitope was detected at different doses, these results were variable. In contrast, little consistent exposure of the HU177 epitope was observed following UVB irradiation of collagen type-I at doses between 0.025J/cm^2 and 5.0J/cm^2. In a similar set of experiments, we assessed the impact of UVA on exposure of the HU177 epitope within interstitial collagen type-I. Interestingly, little consistent exposure of the HU177 epitope was observed within collagen type-I between the UVA doses of 0.1J/cm^2 and 1.0J/cm^2. While exposure of the HU177 epitope was detected within collagen type-I at doses of 2.0J/cm^2 and 5.0J/cm^2, this exposure was inconsistent and variable. The variation in the extent of exposure of the HU177 cryptic epitope in collagen type-I may be a result of time and/or temperature dependent refolding of the triple helical confirmation of the collagen in solution under the experimental conditions tested.

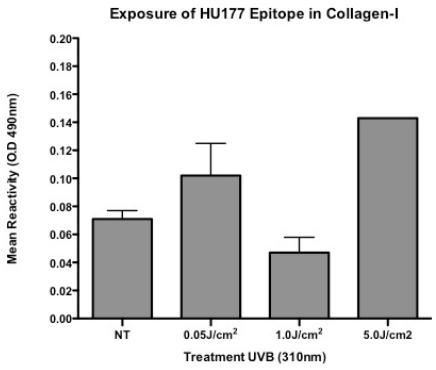

Figure 1. UV-mediated exposure of the HU177 cryptic collagen epitope within collagen in vitro. Human collagen type-I (1.0mg/ml) was either untreated or irradiated with UVB over the dose range indicated and collagen was coated on microtiter wells (0.5ug/ml). Exposure of the HU177 cryptic epitope was detected by solid phase ELISA. Data bars represent the mean Mab D93 reactivity (Optical Density O.D) ± standard deviations from triplicate wells.

Figure 2. UV-mediated exposure of the HU177 cryptic epitope within collagen type-IV in vitro. Using a similar set of experimental approaches as describe above, we examined the exposure of the HU177 epitope within basement membrane collagen type-IV over a dose range (0.05J/cm^2-5.0J/cm^2) of UVA (365) and UVB (310nm) irradiation. As shown in figure 2A, irradiation of collagen type-IV with doses of UVA at 1.0Jcm^2 and 5.0J/cm^2 resulted in extensive exposure of the HU177 cryptic collagen epitope, while little consistent exposure was detected at 0.5J/cm^2. Interestingly, exposure of the HU177 epitope was also detected within collagen type-IV following UVB irradiation at a dose of 1.0J/cm^2 but surprisingly, not at lower doses (0.05J/cm^2) or higher doses (5.0J/cm^2) (Figure 2B). The narrow dose range of UVB capable of exposing the HU177 epitope within

collagen type-IV suggests that specific doses of UV-irradiation may cause limited conformational changes or may destroy the epitope under the experimental conditions tested. Again variation in the extent of exposure was observed especially at low (<0.1J/cm^2) and high doses (> 5.0J/cm^2). As mentioned above, the variation in the extent of exposure of the HU177 cryptic epitope may be a result of time and/or temperature dependent refolding of the triple helical confirmation of the collagen in solution under the experimental conditions tested.

A.

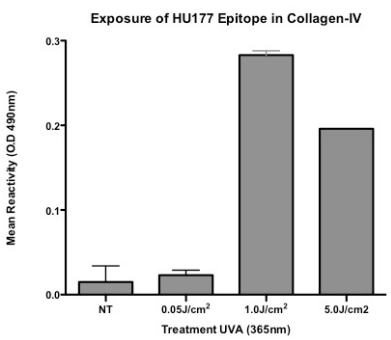

B.

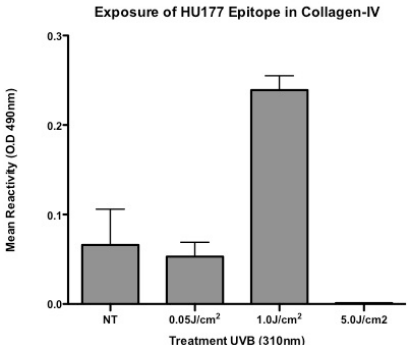

Figure 2. UV-mediated exposure of the HU177 cryptic collagen epitope within collagen in vitro. Human collagen type-IV (1.0mg/ml) was either untreated or irradiated with UVA (A) or UVB (B) over the dose range indicated and collagen was coated on microtiter wells (0.5ug/ml). Exposure of the HU177 cryptic epitope was detected by solid phase ELISA. Data bars represent the mean Mab D93 reactivity (Optical Density O.D) $\pm$ standard deviations from triplicate wells.

Figure 3. Alterations of melanoma cell interactions with UV-irradiated collagen in vitro. Our studies on the effects of distinct UV wavebands on the exposure of the HU177 cryptic collagen epitope indicated that UVA and UVB have differential ability to trigger exposure of the HU177 epitope within both collagen type-I and collagen type-IV. These data suggest that solar irradiation may exhibit a differential capacity to exposure the HU177 epitope within sun-exposed sub-compartments within the skin. However, little is known concerning the impact of UV-irradiated collagen has on the adhesion of distinct cell types. In this regard, we began to examine the effect of UV-mediated exposure of the HU177 epitope might have the capacity of distinct cell types to bind interstitial collagen type-I and basement membrane collagen type-IV. Following extensive testing to establish optimal experimental adhesive conditions, we begin to examine the impact of UV- triggered alterations in collagen structure might have on cellular adhesion to collagen and we initially focused on collagen irradiated with either 0.05J/cm^2 or 5.0J.cm^2. As shown in figure 3A, M21 melanoma cell adhesion to collagen-I was enhanced by nearly 40% following UVA irradiation with a dose as low as 0.05J/cm^2. In similar studies a dose dependent enhancement (greater than 50%) of M21 melanoma cell adhesion to collagen type-I was also observed following UVB irradiation (Figure 3B). To examine whether similar enhancement of melanoma cell adhesion occurs following UV-irradiation of collagen type-IV similar experiments were carried out. As shown in figure 3C, UVA irradiation resulted in a dose dependent enhancement of melanoma cell adhesion to collagen type-IV. Interestingly, while a dose 0.05J/cm^2 of UVA enhanced M21 melanoma cell adhesion to collagen type-IV, low dose (0.05J/cm^2) UVB failed to enhance M21 melanoma cell adhesion to collagen type-IV but 5.0J/cm^2 of UVB enhanced adhesion by approximately 50% (figure 3D). These findings suggest that distinct wavebands of UV irradiation may differentially impact the ability of melanoma cells to interact with distinct types of collagen. Current studies are now underway to examine whether the enhanced melanoma cell adhesion is dependent on specific exposure of the HU177 cryptic collagen epitope.

A.

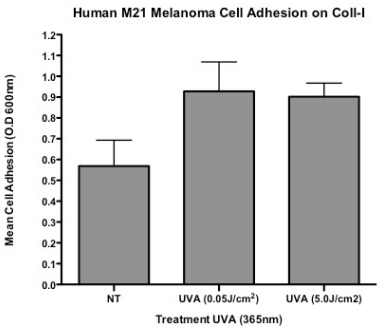

B.

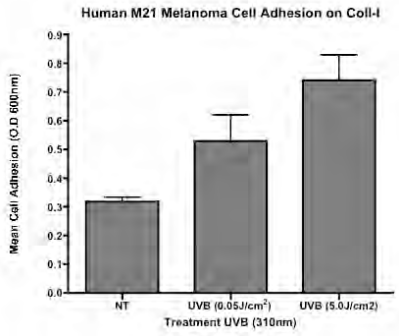

C.

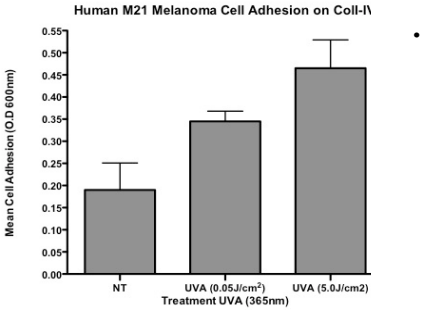

D.

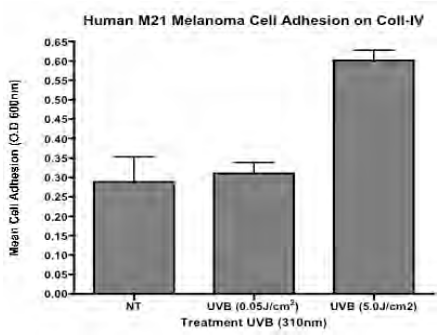

Figure 3. Alterations of melanoma cell interactions with UV-irradiated collagen in vitro. Non-treated and irradiated human collagen type-I (A and B) or collagen type-IV (C and D) were coated on wells and blocked with BSA in PBS. M21 melanoma cells were seeded on the wells and allowed to attach for 15 minutes as we previously described (1-3). Data bars represent mean cell adhesion (Optical Density O.D) $\pm$ standard deviations from triplicate wells.

Figure 4. Alterations of dermal fibroblast cell interactions with UV- irradiated collagen in vitro. The initiation and progression of melanoma has been suggested to involve additional cell types other than the melanoma cells themselves (8-10). Given our studies indicating that melanoma cell interactions with collagen type-I and IV can be differentially and dose dependently enhanced following UV-irradiation, we next examined the effects of UV-irradiated collagen might have on dermal fibroblast cell adhesion. Using similar experimental approaches we coated microtiter wells with UVA or UVB irradiated collagen type-I or type-IV and examined human dermal fibroblast cell adhesion. As shown in figure 4A, fibroblast adhesion to collagen type-I following either low dose (0.05J/cm^2) or a high dose (5.0J/cm^2) UVA irradiation was only slightly (approximately 22%) enhanced as compared to adhesion to non-irradiated collagen. A similar approximately 25% enhancement of fibroblast adhesion was observed on collagen type-I following UVB irradiation at either low or high dose UVB (figure 4B). In contrast to the small increase in fibroblast adhesion to UV-irradiated collagen type-I, UVA irradiation of collagen type-IV at a dose of 5.0J/cm^2 enhanced fibroblast adhesion to collagen IV by over 40% as compared to non-irradiated collagen (Figure 4C). A similar increase (approximately 40%) in fibroblast adhesion to type-IV collagen was also observed following UVB irradiation at a dose of 5.0J/cm^2 (figure 4D). These data are consistent with our previous results indicating the UV-irradiation results in differential and dose dependent alterations in cell adhesion to distinct forms of collagen. Current studies are continuing to examine whether the enhanced fibroblast cell adhesion to collagen type-IV is dependent on specific exposure of the HU177 cryptic collagen epitope.

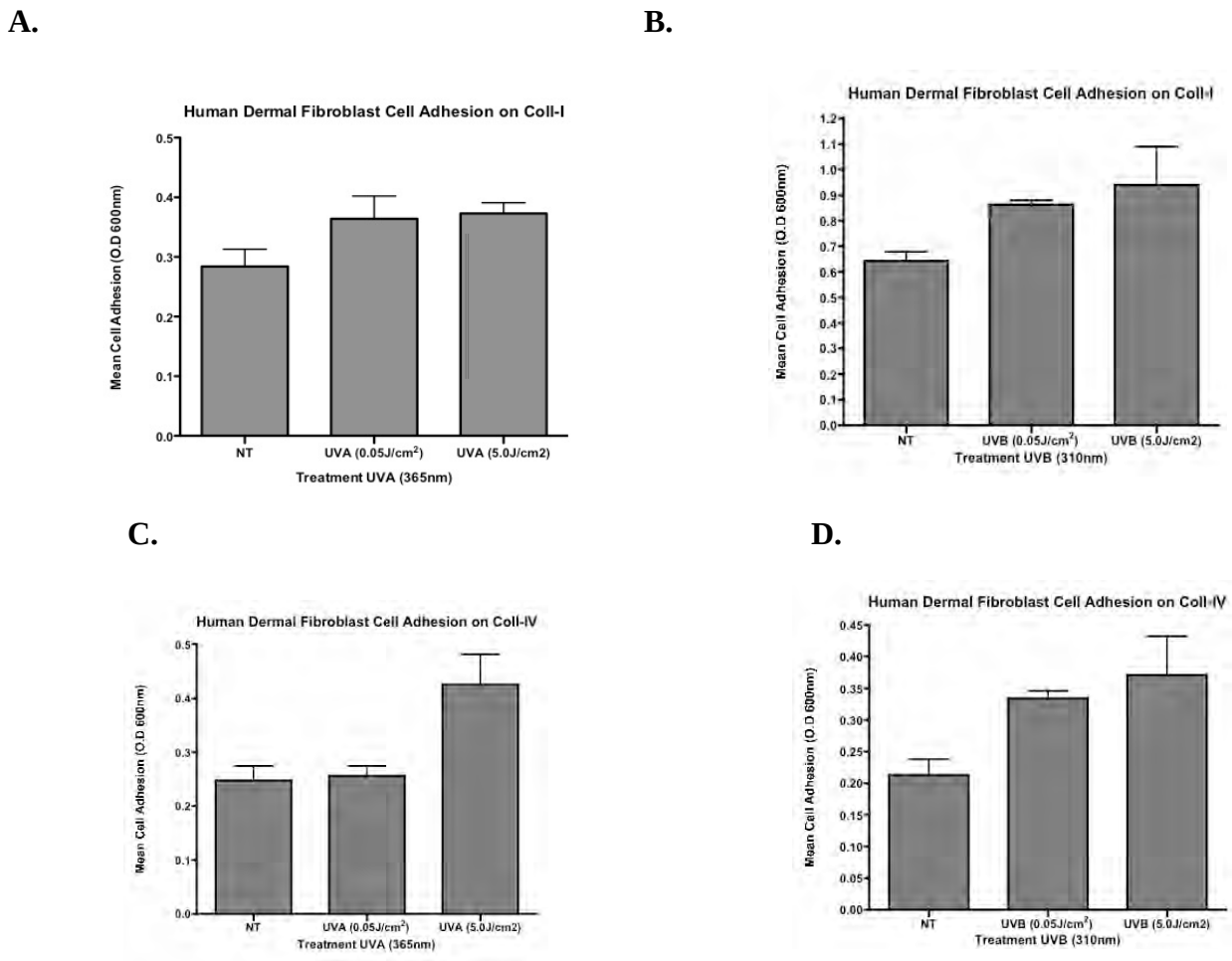

Figure 4. Alterations of fibroblast interactions with UV-irradiated collagen in vitro. Non-treated and irradiated human collagen type-I (A and B) or collagen type-IV (C and D) were coated on wells and blocked with BSA in PBS. Human dermal fibroblasts were seeded on the wells and allowed to attach for 15 minutes as we previously described (1-3). Data bars represent mean cell adhesion (Optical Density O.D) $\pm$ standard deviations from triplicate wells.

Figure 5. Alterations of macrophage interactions with UV-irradiated collagen in vitro. To further examine the impact of UV-irradiation of collagen has of adhesion of distinct cell types that may play a role in melanoma tumor initiation and progression, we evaluated the effects of UV-irradiation has on adhesion of macrophage cell line (Raw 264.7) to collagen type-I and collagen type-IV. In a preliminary experiment collagen type-I and type-IV was irradiated with UVB at a dose of 5.0J/cm^2 and adhesion of murine RAW 264.7 macrophages was assessed. As shown in figure 5A, UVB-irradiation (5.0J/cm^2) had minimal if any effect on macrophage cell adhesion to collagen type-I as compared to non-irradiated collagen. Interestingly, similar UVB irradiation (5.0J/cm^2) of collagen type-IV dramatically enhanced macrophage adhesion by over 5-fold as compared to non-irradiation collagen (figure 5B). While clearly preliminary, these data suggest that UVB irradiation of collagen type-IV, but not collagen type-I may result in a dramatic enhancement of macrophage adhesion to basement membrane collagen type-IV. Additional experiments will be needed to confirm these studies.

Figure 5A.

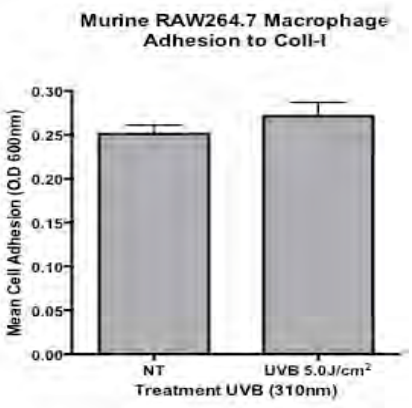

B.

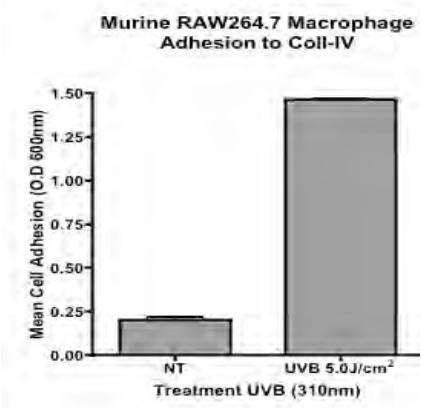

Figure 5. Alterations of macrophage interactions with UV-irradiated collagen in vitro. Non-treated and irradiated human collagen type-I (A) or collagen type-IV (B) were coated on wells and blocked with BSA in PBS. Murine RAW 264.7 macrophage were seeded on the coated wells and allowed to attach for 15 minutes as we previously described (1-3). Data bars represent mean cell adhesion (Optical Density O.D) $\pm$ standard deviations from triplicate wells.

Figure 6. UVA-irradiation of collagen type-I alters human M21 melanoma and fibroblast adhesion. Our previous studies suggested that structural changes induced by UVB-irradiation (310nm) of collagen type-IV, but not collagen type-I could differentially impact cell adhesive behavior in vitro. To examine whether the longer wavelength UVA (365nm) could alter behavior of human melanoma cells and human dermal fibroblasts, cell adhesion assays were carried out with collagen type-I that was not irradiated or irradiated with UVA over a dose range (0 to 5.0J/cm^2). As shown in figure 6A, M21 melanoma cells exhibited an approximately 50% increase in their ability to adhere to collagen type-I irradiated with UVA at a dose of 5.0J/cm^2, while little impact was observed at lower doses. The ability of fibroblast to attach to UVA irradiated collagen type-I was only marginally enhanced (figure 6B). These data are consistent with our previous studies indicating a dose and cell type specific alteration in cell adhesive behavior following UV irradiation.

A. **B.**

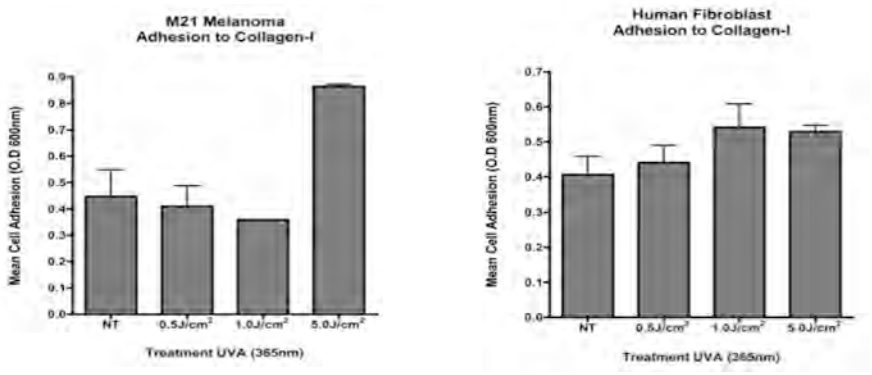

Figure 6. Alterations of cell interactions with UVA-irradiated collagen type-I. Non-treated and irradiated collagen type-I were coated (5.0ug/ml) on wells and blocked with BSA. A). M21 melanoma cells or B) human dermal fibroblasts were seeded on the wells and allowed to attach as we described (1-3). Data bars represent mean cell adhesion (Optical Density O.D) ± standard deviations from triplicate wells.

Figure 7. UVA-irradiation of collagen type-IV differentially alters human M21 melanoma and fibroblast adhesion. Given our studies suggesting UVA irradiation of collagen type-I may alter cell adhesion, we carried out similar studies using basement membrane collagen type-IV. As shown in figure 7A, a small increase in M21 melanoma cell adhesion to UVA-irradiated collagen type-IV at a dose of 0.5 and 1.0J/cm^2, while little impact was observed at 5.0J/cm^2. The ability of fibroblasts to attach to UVA irradiated collagen type-IV was also marginally enhanced at 5.0J/cm^2 (figure 7B).

A. **B.**

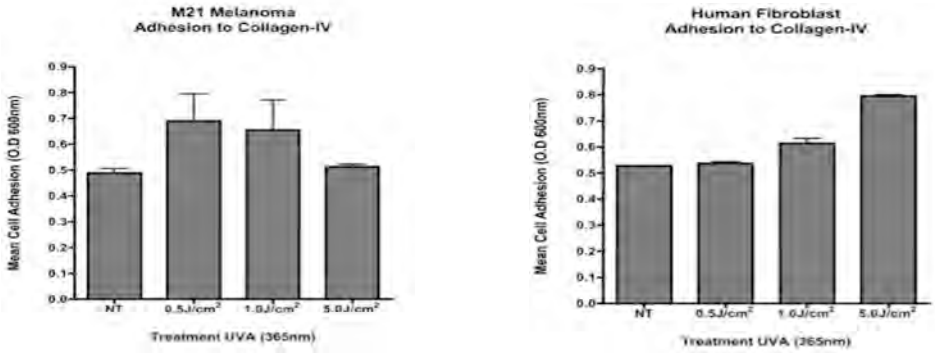

Figure 7. Alterations of cell interaction with UVA-irradiated collagen type-IV. Non-treated and irradiated collagen type-IV were coated (5.0ug/ml) on wells and blocked with BSA. A). M21 melanoma cells or B) human dermal fibroblasts were seeded on the wells and allowed to attach as we described (1-3). Data bars represent mean cell adhesion (Optical Density O.D) ± standard deviations from triplicate wells.

Figure 8. UVA-irradiation of collagen type-I differentially alters human melanoma and fibroblast proliferation in vitro. To assess the effects of UVA irradiation of collagen type-I on melanoma and fibroblast cell growth in vitro, we carried out in vitro proliferation assays. Briefly, interstitial collagen type-I was either untreated or irradiated with UVA over a dose range (0-5.0 J/cm^2) and proliferation was assessed over a time course (0-72hrs). Little change in the proliferation of either M21 melanoma or fibroblasts was observed under the experimental conditions within the first 48hrs. However, as shown in figure 8A, a small reduction was observed in M21 melanoma cell growth on UVA (0.5J/cm^2) irradiated collagen by day 3. In contrast, an approximately 50% increase in fibroblast cell growth was observed by day 3 on UVA irradiated collagen type-I at a dose of 0.5J/cm^2 or higher (figure 8B).

A. **B.**

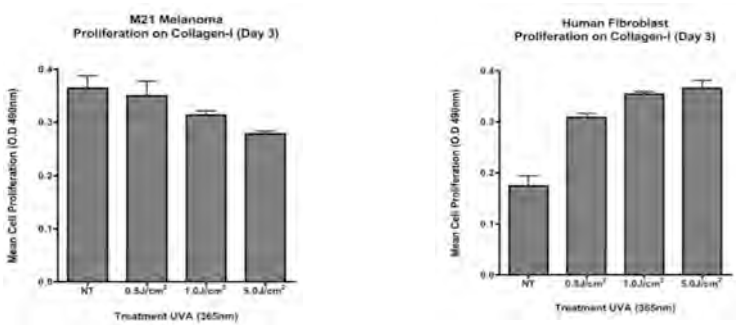

Figure 8. UVA-irradiation of collagen type-I alters melanoma and fibroblast growth in vitro. Collagen type-I was not treated or irradiated with UVA (365nm) over a dose range (0-5.0J/cm^2). Wells were coated (5.0ug/ml) with untreated or UVA treated collagen and M21 melanoma cells (A) or human dermal fibroblasts (B) were seeded and allowed to grow over a 3-day time course. Proliferation was monitored using MTT assay. Data bars represent mean proliferation (Optical Density O.D) $\pm$ standard deviations from triplicate wells on Day 3.

Figure 9. UVA-irradiation of collagen type-IV alters human melanoma and fibroblast proliferation in vitro. To assess the effects of UVA irradiation of collagen type-IV on melanoma and fibroblast cell growth in vitro, we carried out proliferation assays essentially as described above. Again, little change in the proliferation of either M21 melanoma or fibroblasts was observed within the first 48hrs. However, as shown in figure 9A, similar to what was observed on collagen type-I, a small reduction was observed in M21 melanoma cell growth on UVA irradiated collagen as compared to control and an approximately 38% increase in fibroblast cell growth was observed by day 3 on UVA irradiated collagen at a dose of 0.5J/cm^2 or higher (figure 9B).

A. **B.**

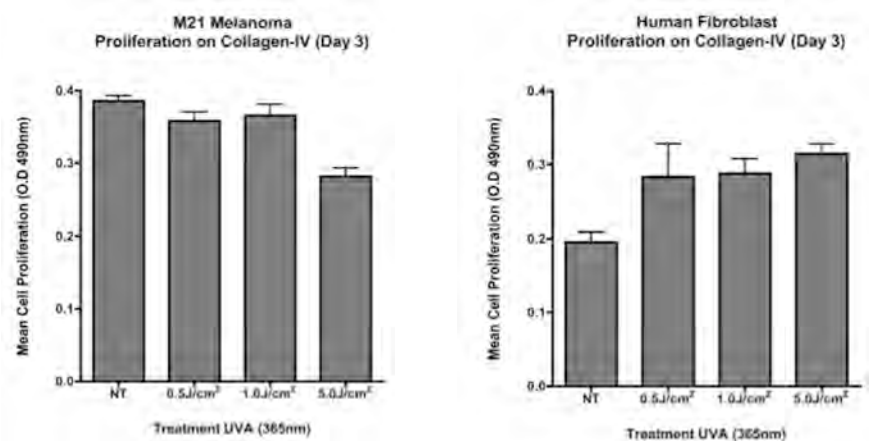

Figure 9. UVA-irradiation of collagen type-IV alters M21 melanoma and fibroblast cell proliferation in vitro. Collagen type-IV was either not treated or irradiated with UVA (365nm) over a dose range (0-5.0J/cm^2). Microtiter wells were coated (5.0ug/ml) with untreated or UVA treated collagen and M21 melanoma cells (A) and human dermal fibroblasts (B) were seeded in wells and allowed to grow over a 3-day time course. Proliferation was monitored using MTT assay. Data bars represent mean proliferation (Optical Density O.D) $\pm$ standard deviations from triplicate wells.

Figure 10. Exposure of the HU177 cryptic epitope within Matrigel^{TM} in vitro. To begin to assess whether specific UV wavebands my trigger exposure of the HU177 epitopes within Matrigel^{TM}, a secreted basement membrane-like ECM composed predominately of laminin and collagen type-IV, we irradiated Matrigel^{TM} with

UVB over a dose range (0-5J/cm^2). Solid phase ELISA assays were carried out to assess the relative exposure of the HU177 epitope. Surprising, the HU177 epitope could be detected in non-irradiated Matrigel^{TM} (Figure 10). Interestingly, while a small enhancement of reactivity could be detected following UVB irradiation at a dose of 0.5J/cm^2, a dose of 5.0J/cm^2 reduced reactivity with anti-HU177 antibody. These data suggest that the HU177 cryptic collagen epitope appears to be exposed within Matrigel^{TM} prior to UV-irradiation and that collagen type-IV present within Matrigel^{TM} is at least partially in a non-triple helical conformation.

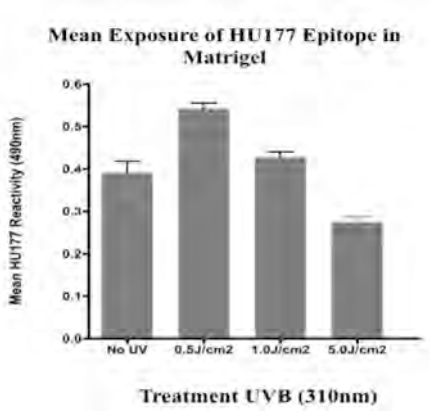

Figure 10. UV-mediated exposure of the HU177 cryptic collagen epitope within Matrigel^{TM} in vitro. Matrigel^{TM} was untreated or irradiated with UVB over the dose range indicated and coated on microtiter wells. Exposure of the HU177 cryptic epitope was detected by solid phase ELISA. Data bars represent the mean Mab D93 reactivity (Optical Density O.D) $\pm$ standard deviations from triplicate wells.

Figure 11. Differential adhesion of human M21 melanoma cells and dermal fibroblasts to UVB-irradiated Matrigel^{TM}. Given our previous studies suggesting differentially enhanced melanoma cell adhesion to UV-irradiated collagen I and IV, we examined the effects of UV-irradiation on cell adhesion to basement membrane preparation Matrigel^{TM}. Matrigel^{TM} was irradiated with UVB over a dose range from 0-5.0J/cm^2. Surprisingly, as shown in figure 11A, human M21 melanoma cell adhesion to UVB-irradiated Matrigel^{TM} was inhibited by nearly 40% at 5.0J/cm^2. In contrast, dermal fibroblast adhesion was enhanced dose dependently, exhibiting a maximum enhancement at a UVB dose of 1.0J/cm^2 (figure 11B).

A. **B.**

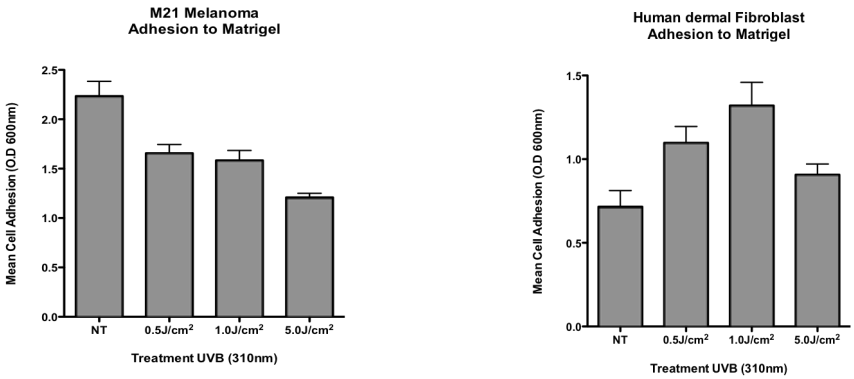

Figure 11. Alterations of melanoma cell interactions with UV-irradiated Matrigel^{TM}. Non-treated and irradiated Matrigel^{TM} were coated on wells and blocked with BSA in PBS. A). M21 melanoma cells or B) human dermal fibroblasts were seeded on the wells and allowed to attach as we previously described (1-3). Data bars represent mean cell adhesion (Optical Density O.D) $\pm$ standard deviations from triplicate wells.

Figure 12. Differential adhesion of human M21 melanoma cells and dermal fibroblasts to UVA-irradiated Matrigel^{TM}. Given the differential impact of UVB-irradiated Matrigel^{TM} had on cell adhesion, we examined the effects of UVA-irradiation on cell adhesion to Matrigel^{TM} using a similar assay. Matrigel^{TM} was irradiated with UVA over a dose range from 0-5.0J/cm^2. Surprisingly, in contrast to UVB (figure 12A), M21 melanoma cell adhesion to UVA-irradiated Matrigel^{TM} was enhanced by greater than 50% at 0.5J/cm^2 or higher as compared to control. In addition, human dermal fibroblast adhesion was enhanced by nearly 40%, at

a UVA dose of 5.0J/cm^2 (figure 12B). These important studies indicate the complex and potentially opposing effects of UVA as compared to UVB on cell adhesive behavior.

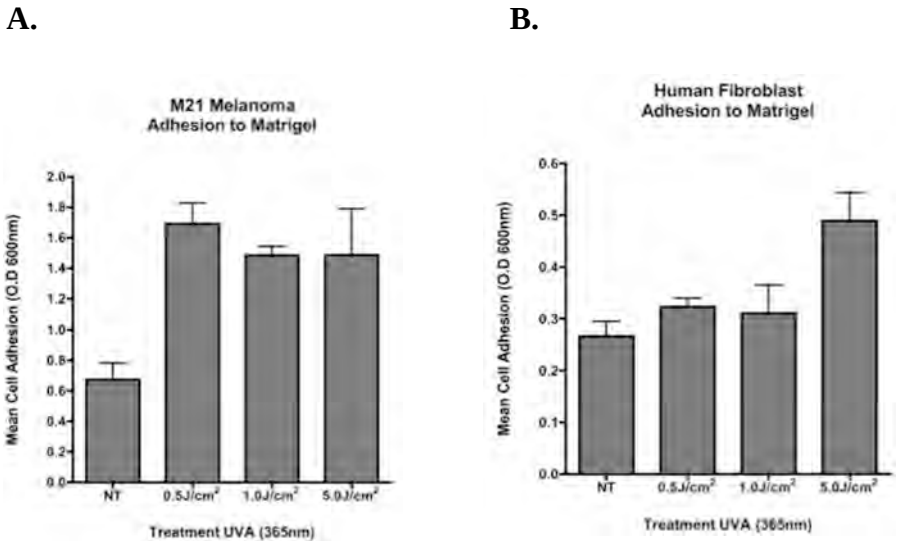

Figure 12. Alterations of melanoma cell interactions with UVA-irradiated Matrigel™. Non-treated and irradiated Matrigel™ were coated (5.0ug/ml) on wells and blocked with BSA. A). M21 melanoma cells or B) human fibroblasts were seeded on the wells and allowed to attach as we previously described (1-3). Data bars represent mean cell adhesion (Optical Density O.D) ± standard deviations from triplicate wells.

Figure 13. UVA-irradiation of Matrigel™ differentially alters human melanoma and fibroblast proliferation in vitro. To assess the effects of UVA irradiated Matrigel™ on melanoma and fibroblast growth in vitro, we carried out in vitro proliferation assays. Briefly, Matrigel™ was either untreated or irradiated with UVA over a dose range (0-5.0 J/cm^2) and proliferation was assessed over a time course (0-72hrs). Little change in the proliferation of either M21 melanoma or fibroblasts was observed under the experimental conditions within the first 48hrs. However, as shown in figure 13A, a small reduction was observed in M21 melanoma cell growth on UVA irradiated Matrigel™ as compared to control by day 3. In contrast, an approximately 50% increase in fibroblast growth was observed by day 3 at a dose of 0.5J/cm^2 or higher (figure 13B).

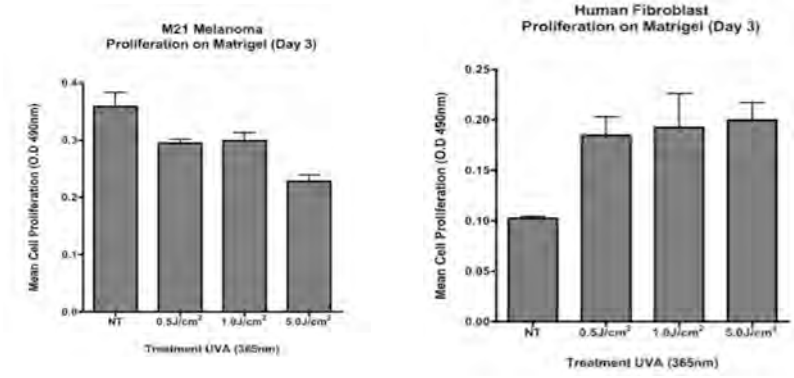

Figure 13. UVA-irradiation of Matrigel™ alters M21 melanoma and fibroblast proliferation in vitro. Matrigel™ was either not treated or irradiated with UVA (365nm) over a dose range (0-5.0J/cm^2). Microtiter wells were coated (5.0ug/ml) with untreated or UVA treated Matrigel™ and M21 melanoma cells (A) and dermal fibroblasts (B) were seeded in wells and allowed to grow over a 3-day time course. Cell proliferation was monitored using MTT assay. Data bars represent mean cell proliferation (Optical Density O.D) ± standard deviations from triplicate wells.

Figure 14. Differential migration of M21 melanoma cells and Raw 264.7 macrophages on UV-irradiated Matrigel™. Given our previous studies, we examined the effects of UV-irradiation on cell migration on Matrigel™. Matrigel™ was irradiated with UVB over a dose range from 0-5.0J/cm^2 and M21 melanoma cells or Raw 264.7 macrophages were allowed to migrate using Matrigel™ coated transwell migration chambers. As shown in figure 14A, enhanced migration of M21 melanoma cells was detected on Matrigel™ irradiated at a dose of 0.5J/cm^2, while little change was detected in migration on Matrigel™ irradiated at higher doses. In

contrast, reduced macrophage migration was observed on Matrigel™ irradiated with increasing doses of UVB (figure 14B). These data again confirm the complex cell type and dose-dependent changes in cellular behavior that occur as a result of UV-mediated structural alteration of ECM proteins in vitro.

A. **B.**

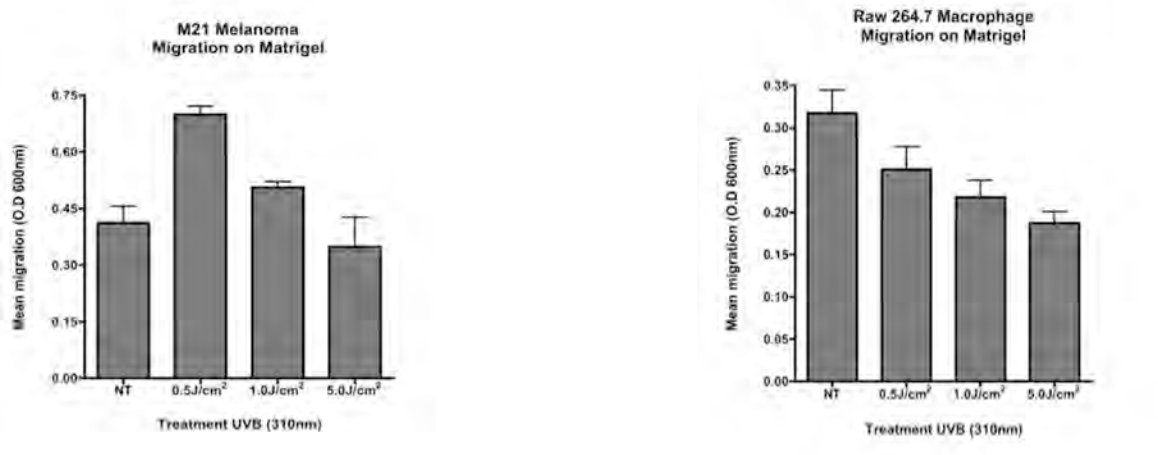

Figure 14. Differential migration of M21 melanoma cells and Raw 264.7 macrophages on UV-irradiated Matrigel™. Non-treated and irradiated Matrigel™ (5.0ug/ml) were coated on membranes of transwell migration chambers. Sub-confluent cells were resuspended in migration buffer and seeded in the upper chamber. A). Quantification of M21 melanoma cells migration. B) Quantification of Raw 264.7 macrophage migration. Data bars represent mean cell migration (Optical Density O.D) ± standard deviations from triplicate wells.

Figure 15. UVB-irradiation of Matrigel™ fails to alter M21 melanoma cell proliferation in vitro. To assess the effects of UVB irradiation of Matrigel™ on melanoma cell growth in vitro, we carried out in vitro proliferation assays. Briefly, Matrigel™ was either untreated or irradiated with UVB over a dose range (0-5.0 J/cm^2) and proliferation was assessed over a time course (0-72hrs). As shown in figure 15A-C, UVB irradiation of Matrigel™ failed to significantly alter M21 melanoma cell proliferation over the time course tested. These findings suggest that while UVB irradiation of Matrigel™ alters melanoma cell adhesion, it caused little if any change on their ability to grow over the 3-day time course.

A. **B.** **C.**

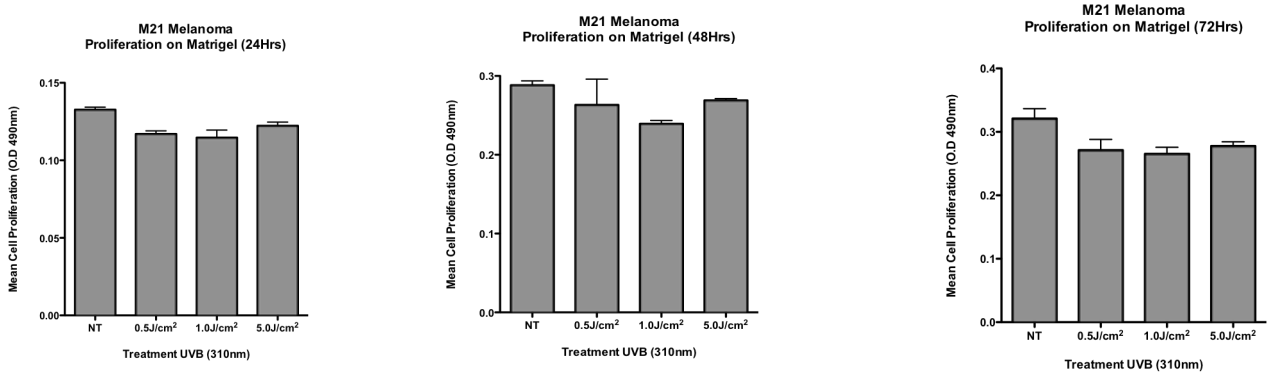

Figure 15. UVB-irradiation of Matrigel™ fails to alter M21 melanoma cell proliferation in vitro. Matrigel™ was either not treated or irradiated with UVB (310nm) over a dose range (0-5.0J/cm^2). Microtiter wells were coated (5.0ug/ml) with untreated or UVB treated Matrigel™ and M21 melanoma cells were seeded in wells and allowed to grow over a 3-day time course. Tumor cell proliferation was monitored using MTT assay. Data bars represent mean cell proliferation (Optical Density O.D) ± standard deviations from triplicate wells.

Figure 16. UVB-irradiation of collagen type-IV enhances murine macrophage migration. Our previous studies suggested that UVB-irradiation of collagen type-IV, but not collagen type-1 could enhance macrophage adhesion. These findings are consistent with the possibility that UVB irradiation induces a structural change in collagen type-IV that facilitates enhanced adhesion. In this regard, we examined whether UVB-mediated structural change in collagen type-IV could also enhance macrophage migration. To examine this possibility, Raw 264.7 macrophages were allowed to migrate on transwells coated with either untreated or UVB-treated (5.0J/cm^2) collagen type-I or collagen type-IV. As shown in figure 16A, macrophages exhibited similar migratory capacity on either untreated or UVB-irradiated collagen type-I. In contrast, macrophage exhibited enhanced migration on UVB-irradiated collagen type-IV as compared to untreated collagen type-IV (figure 16B). These data are consistent with our previously reported adhesion data and suggest that a unique UVB-mediated structural change in collagen type-IV, but not collagen type-I enhances macrophage migration.

A **B.**

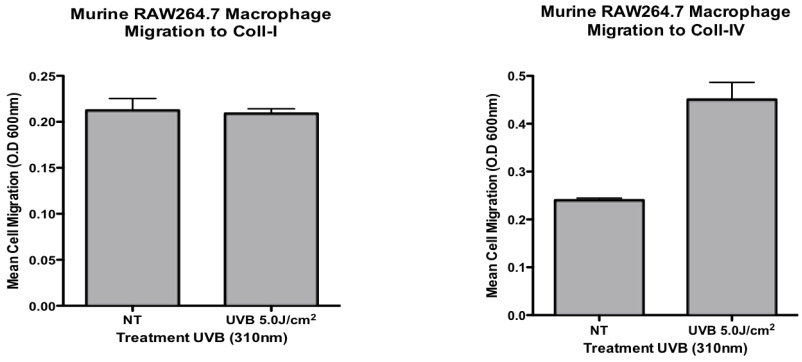

Figure 16. Alterations of macrophage interactions with UV-irradiated collagen-IV Non-treated and UVB irradiated (5.0J/cm^2) collagen type-I (A) and collagen type-IV (B) were coated (5.0ug/ml) on membranes of transwell migration chambers. RAW 264.7 macrophages were seeded and allowed to migrate as we described (1-3). Data bars represent mean cell migration (Optical Density O.D) $\pm$ standard deviations from triplicate wells.

Figure 17. UVB-irradiation of collagen type-IV enhances macrophage proliferation in vitro. Given the consistent findings indicating that UVB-mediated structural change in collagen type-IV alters the adhesive and migratory behavior of macrophages on this ECM substrate, we assessed the effects of UVB irradiation of collagen type-IV on macrophage growth in vitro. Briefly, collagen type-IV was either untreated or irradiated with UVB (5.0 J/cm^2) and proliferation was assessed over a time course (0-72hrs). As shown in figure 17A-C, UVB irradiation of collagen type-IV enhanced proliferation by approximately 30% to 40% over the time course tested. These findings are consistent with UVB-mediated structural change in collagen type-IV altering the behavior of macrophages in vitro.

A. **B.** **C.**

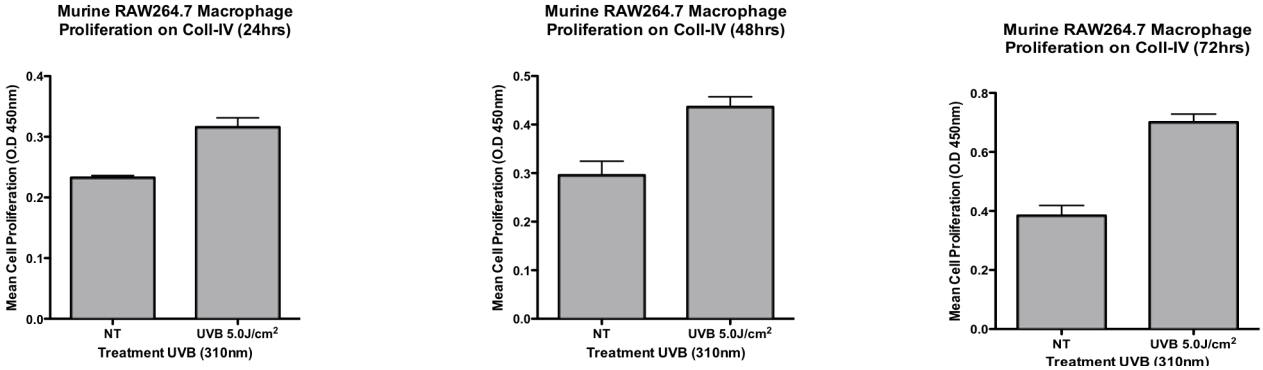

Figure 17. UVB-irradiation of collagen type-IV alters macrophage proliferation in vitro. Collagen type-IV was either not treated or irradiated (0-5.0J/cm^2) with UVB (310nm). Microtiter wells were coated (5.0.0ug/ml) with untreated or UVB treated collagen and murine macrophages were seeded in wells and allowed to grow over a 3-day time course. Proliferation was monitored using MTT assay. Data bars represent mean cell proliferation (Optical Density O.D) $\pm$ standard deviations from triplicate wells.

Figure 18. UV-mediated induction of inflammatory cells in mouse skin. To begin to establish a time course and dose of UV irradiation needed to induce a reproducible inflammatory response in full thickness mouse skin, mice were irradiated with UVB over a dose range of 0-1.0J/cm^2 and skin has harvested 24hrs, 48hrs and 72hrs later. The full thickness skin was either snap frozen or embedded in paraffin and tissues sections prepared. To examine the tissues for inflammatory infiltrates the tissues were stained by Giemsa. As shown in figure 18A middle panel, UVB at a dose of 0.1J/cm^2 induced infiltration of inflammatory cells (arrows) primarily confined to the subcutaneous fat with minor infiltration into the lower regions of the dermis by 24 hours as compared to non-UV (left panel). UVB irradiation with a dose of 1.0Jcm^2 (right panel) induced a strong inflammatory infiltrate into the middle and upper levels of the dermis (Rights panel). Little over all changes could be detected in the relative levels inflammatory infiltrates between 48 and 72 hours following UV irradiation (figure 18B an C). Under these conditions, our data suggests that UVB irradiation at either 0.1Jcm^2 or 1.0Jcm^2 induces a significant inflammatory infiltrate.

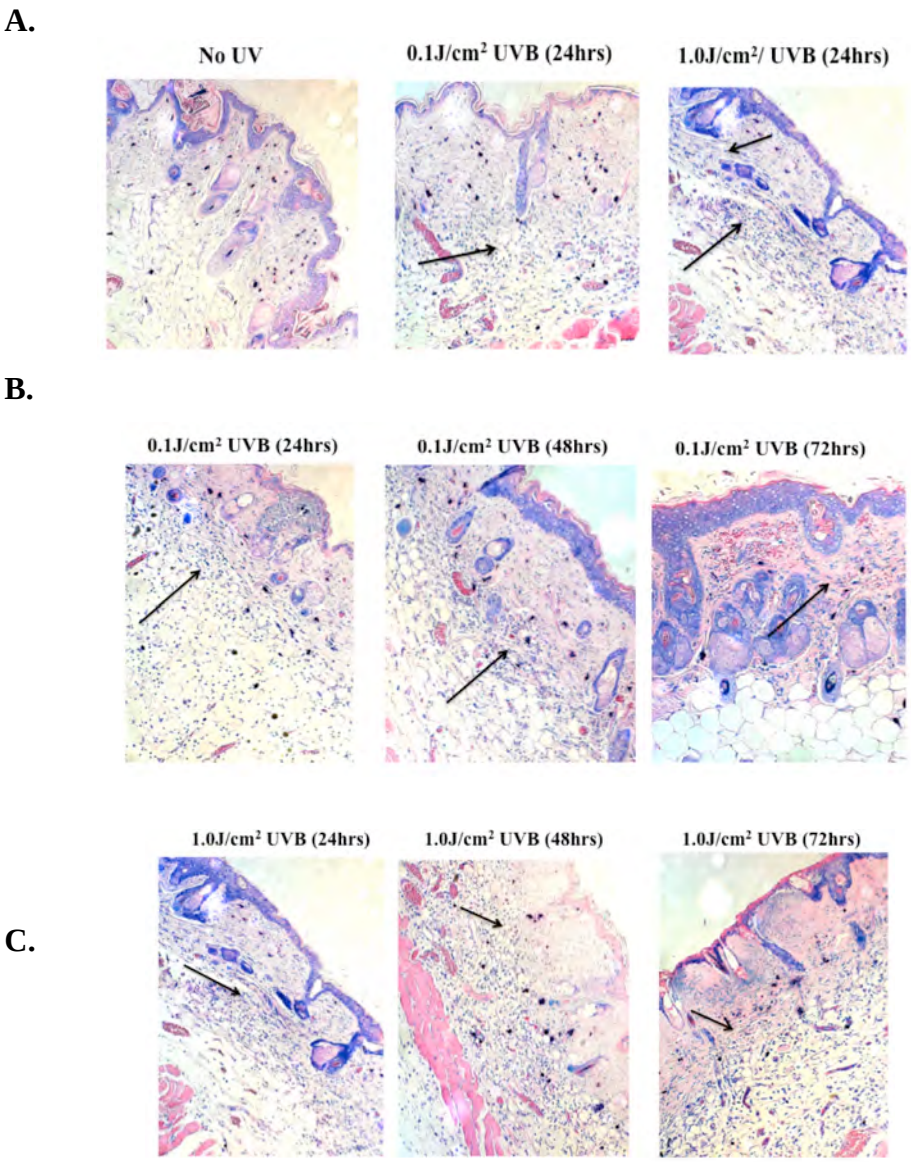

Figure 18. UV-mediated induction of inflammatory cells in mouse skin. Mice (nude) were either not treated or irradiated (0.1-1.0J/cm^2) with UVB (310nm). Mice were sacrificed over a time course of 3 days (24hrs, 48hrs or 72hrs) and full thickness skin was harvested and embedded in paraffin. Tissue sections were cut and stained by Giemsa method to detect immune cells (arrows). Small blue cells include neutrophils, larger cells with characteristic large nuclei include macrophages, and dark purple granulated cells include mast cells. A). Representative examples of mouse skin from either untreated left panel (No UV) or UVB-irradiated middle panel (UVB 0.1J/cm^2), or right panel (UVB 1.0J/cm^2). B). Representative examples of mouse skin from UVB- irradiated (0.1J/cm^2) left panel (24hrs) or middle panel (48hrs), or right panel (72hrs). C). Representative examples of mouse skin from UVB- irradiated (1.0J/cm^2) left panel (24hrs) or middle panel (48hrs), or right panel (72hrs). Black arrows indicate examples of immune infiltrates. All photos taken at a magnification of 100x.

Figure 19. Immunofluorescence detection of elevated neutrophils in UVB-irradiated mouse skin. Given our studies establishing the parameters useful for inducing UV-mediated inflammatory cell infiltration into full thickness mouse skin, we began to characterize the types of inflammatory cell infiltrates that were induced by UV-irradiation in this mouse model. Frozen sections of full thickness murine skin from either untreated or UVB irradiated were analyzed for the presence of neutrophils using the previously described murine neutrophil marker (7/4 antigen). As shown in figure 19, few neutrophils could be detected with the epidermis or dermis of non-irradiated skin (left panels). In contrast, 24hrs post UVB irradiation (top panels) a dose dependent increase in neutrophil infiltration (red) could be readily detected. Importantly, 48hrs post UV irradiation, neutrophils persisted following UV-irradiation at 1.0Jcm^2. These data confirm a time and dose dependent infiltration of neutrophils following UVB-irradiation.

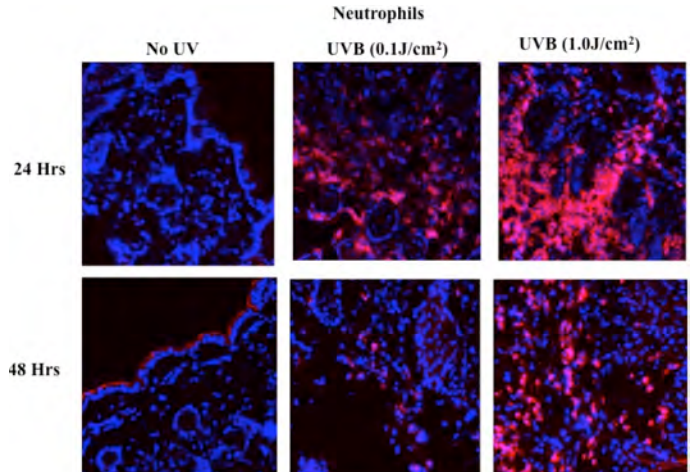

Figure 19. Detection of elevated levels of neutrophils in UVB-irradiated mouse skin. Mice (nude) were either not treated or irradiated (0.1-1.0J/cm^2) with UVB (310nm). Mice were sacrificed at 24hr and 48hrs and full thickness skin was harvested and embedded. Tissue sections were cut and stained for the presence of infiltrating neutrophils. Red color indicates neutrophils (7/4 antigen) and blue indicated Dapi. All photos taken at a magnification of 200x.

Figure 20. Immunofluorescence detection of macrophages in UVB-irradiated mouse skin. Given our studies suggesting elevated neutrophil infiltration following UVB-irradiation, we examine murine skin for the presence of macrophages. In contrast to neutrophils, macrophages could be detected in normal non-irradiated skin and by 48hrs post UV-irradiation some enhancement of the relative levels of macrophages could be detected at 1.0J/cm^2, however little change was detected at lower doses of UVB-irradiation or at earlier time points (Figure 20). These data, in conjunction with the distinct enhancement of mast cell infiltration purple granulated cells following Giemsa staining) confirm the differential induction of distinct subsets of inflammatory cells following UVB-irradiation of murine skin.

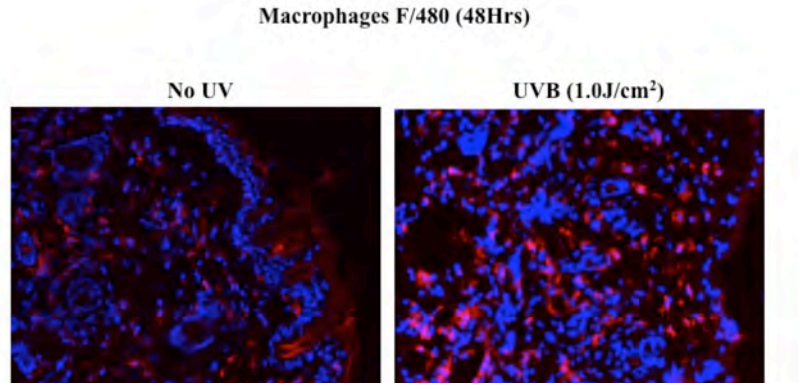

Figure 20. Detection of elevated levels of macrophages in UVB-irradiated mouse skin. Mice (nudes) were either not treated or irradiated (0.1-1.0J/cm^2) with UVB (310nm). Mice were sacrificed at 48hrs and full thickness skin was harvested and embedded. Tissue sections were cut and stained for the presence of macrophages (F4/80 antigen). Red color indicates macrophages and blue indicated Dapi. All photos taken at a magnification of 200x.

Figure 21. Immunofluorescence detection of altered proteolytic enzymes in UVB-irradiated mouse skin. Previous studies have implicated enhanced expression of a number of proteolytic enzymes in activated

neutrophils and macrophages. Our previous studies have suggested that enzymes such as MMPs may contribute to the exposure of cryptic collagen epitopes in vivo. Therefore, we began to examine the expression of enzymes known to be expressed by inflammatory infiltrates including the serine protease neutrophil elastase and the gelatinase MMP-9. As shown in figure 21A, coinciding with the elevated infiltration of neutrophils, enhanced levels of neutrophil elastase could be readily detected predominately within the epidermal and dermal layers by 48hrs following UVB-irradiation (1.0J/cm^2). In similar studies, elevated levels of MMP-9 were also detected with strong staining noted in the epidermis and surrounding dermal blood vessels and scattered dermal cells (Figure 21B). These data confirm enhanced levels of proteolytic enzymes, which might contribute to the exposure of the HU177 epitope in vivo following UVB irradiation.

A. **B.**

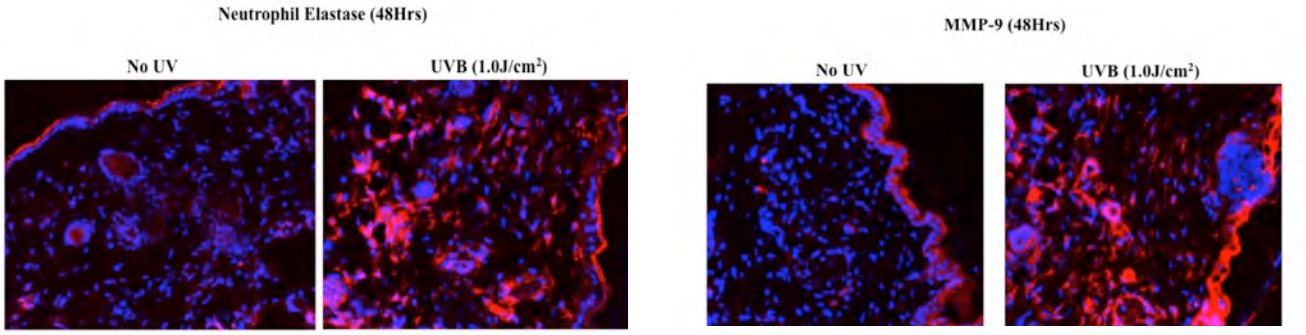

Figure 21. Detection of altered proteolytic enzymes in UVB-irradiated mouse skin. Mice (nude) were either not treated or irradiated (0.1-1.0J/cm^2) with UVB (310nm). Mice were sacrificed at 48hrs and full thickness skin was harvested and embedded. Tissue sections were cut and stained for the presence of Neutrophil Elastase or MMP-9. A). Red color indicates Neutrophil Elastase and Blue indicated Dapi. B). Red color indicates MMP-9 and Blue indicated Dapi All photos taken at a magnification of 200x.

Figure 22. Blocking the HU177 cryptic collagen epitope inhibits UVB-induced mast cell accumulation in skin. Given our studies establishing the experimental parameters useful for inducing UV-mediated inflammatory cell infiltration into full thickness mouse skin, we began to examine the effects of blocking cellular interactions with the HU177 cryptic collagen epitope on UV-mediated mast cell accumulation within skin. Briefly, mice were either untreated or injected with a single i.p injection (100ug/mouse) of function blocking anti-HU177 humanized Mab D93 or non-specific control IgG. Twenty-four hours later mice were either not irradiated or irradiated with UVB (0.1J.cm^2) and full thickness skin was harvested 24hrs later. Tissue sections were prepared as described above and mast cell (dark purple granulated cells) infiltration into the dermis was evaluated following Giemsa staining. Importantly, examination of the tissue sections from each experimental condition suggested a reduction in the relative levels of mast cell accumulation within the dermal regions of the skin of mice pretreated with anti-HU177 humanized Mab D93 as compared to controls (figure 22A). In fact, quantification of the relative levels of mast cells per 200X field indicated a near complete inhibition of UV-induced mast cell accumulation back to levels prior to UVB irradiation, while a non-specific control antibody exhibited minimal change (figure 22B). These exciting new data suggest that the HU177 epitope may play a functional role in UVB-induced mast cell accumulation in the skin.

A. **B.**

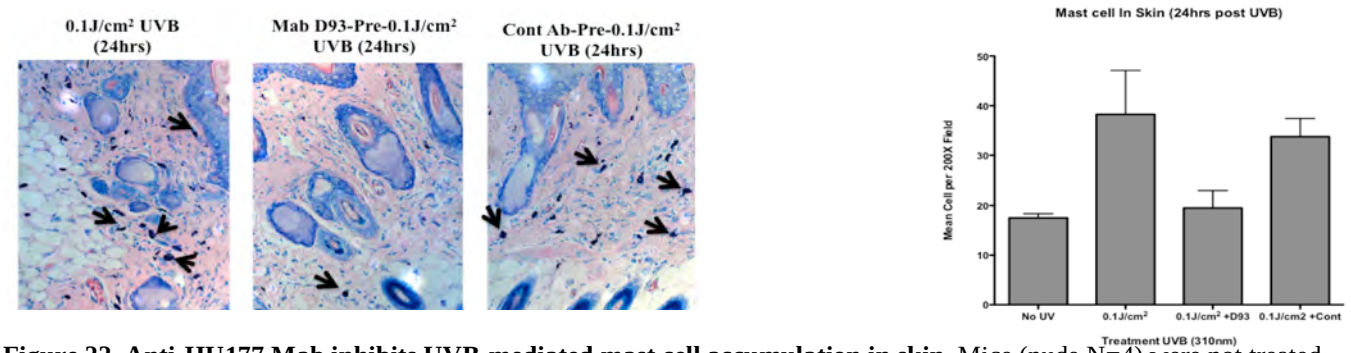

Figure 22. Anti-HU177 Mab inhibits UVB-mediated mast cell accumulation in skin. Mice (nude N=4) were not treated or treated with a single i.p injection of D93 Mab or control (100ug). Twenty-four hours later mice were not irradiated or irradiated (0.1J/cm^2) with UVB. Mice were sacrificed 24hrs later and skin was embedded in paraffin. Tissue sections were cut and stained by Giemsa to detect mast cells (arrows heads). A). Representative examples of mouse skin from UVB 0.1J/cm^2 irradiated (left panel) or pre-treated with Mab D93 and UVB-irradiated (middle panel) or pre-treated with control Ab and UVB-irradiated (Right panel). Dark purple granulated cells at arrows show examples of mast cells. B) Quantification of the mean number of mast cells within the dermal region of the skin. Data bars represent the mean mast cells per 200X field ± Standard Error from 10 independent fields.

Figure 23. UVB irradiation-induced enhancement of melanoma growth depends in part on the HU177 epitope. Given our studies indicating that 0.1J/cm^2 can induced a strong infiltration of inflammatory cells including neutrophils, mast cells and macrophages and these cell types have been suggested to contribute to tumor initiation and growth, we examined the impact of UVB-irradiation on M21 melanoma growth in nude mice. Briefly, mice were either untreated or pre-treated with a single i.p injection of 100ug of anti-HU177 epitope antibody D93. Twenty-four hours later mice were not irradiated or irradiated with a single dose of UVB (310) 0.1J/cm^2. Twenty-four hours later mice were injected subcutaneously with M21 melanoma cells (3x10^6). Melanoma tumor growth was monitored over a time course of 21 days. As shown in figure 23A, a single UVB dose of irradiation resulted in larger tumors as compared to control (NT). Importantly, pretreating the mice prior to UVB-irradiation resulted in smaller tumors as compared to UVB–irradiated mice. In fact, quantification of tumor size indicated that pre-treating mice with a single 100ug injection of anti-HU177 cryptic epitope antibody prior to UVB –irradiation inhibited melanoma tumor growth by nearly 40% as compared to control (figure 23B). These preliminary experiments suggest that UVB-irradiation enhancement of melanoma growth in these mice may be do in part, to the functional exposure of the HU177 cryptic collagen epitope.

A. **B.**

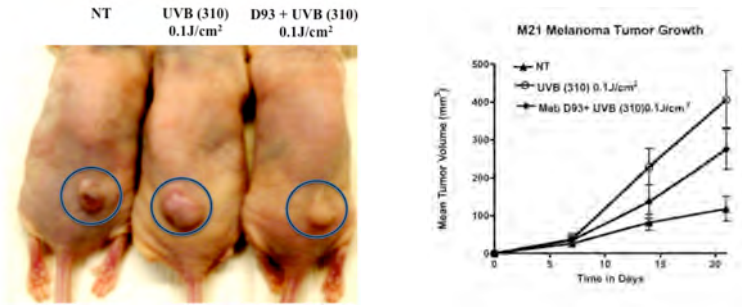

Figure 23. UVB Irradiation-induced enhanced M21 melanoma growth depends in part on the HU177 epitope. Mice (N=5-7) were not treated or injected with a single i.p treatment with anti-HU177 humanized antibody D93 (100ug). Twenty-four hours later mice were not irradiated or irradiated (0.1J/cm^2) with UVB (310nm). Twenty-four hours later, mice were injected subcutaneously with M21 melanoma cells (3x10^6). Mice were sacrificed at day 21. Tumor growth was monitored by caliper measurements. A). Representative examples of mice from either non-treated controls (left panel), UVB 0.1J/cm^2 irradiated (middle panel) or pre-treated with Mab D93 and UVB-irradiated (right panel). B) Quantification of the mean tumor volume from each experimental condition. Data bars represent the mean tumor volume ± Standard Error.

Figure 24. Exposure of the HU177 cryptic epitope in full thickness human skin following ex vivo UV-irradiation. Our previous studies have indicated the UV-irradiation of purified collagen in vitro can result in structural changes that lead to exposure of the HU177 epitope. To begin to characterize the human neonatal foreskin that will be used in the human/mouse chimeric model, we first assessed whether UV-irradiation can also expose the HU177 epitope in full thickness human skin. Briefly, surgical explants of discarded neonatal human foreskin was either not treated or irradiated with UVA and UVB ex vivo at either 0.1J/cm^2 or 1.0J/cm^2. Tissues were either snap frozen or embedded in paraffin and tissues section prepared. To assess basal levels of any inflammatory cells within these human skin samples following surgical resection, tissues were stained by Giemsa. As shown in figure 24A, UV-irradiation of explanted full thickness human skin exhibited few if any inflammatory infiltrates and were similar to untreated control skin since these human skin samples were surgically removed from patients prior to UV-irradiation. The relative levels and distribution of collagen within both non-treated and UV-irradiated human skin were also similar as indicated by trichrome staining (figure 24B). Importantly, while some exposure of the HU177 epitope was detected in these untreated skin specimens, UV-irradiation of these surgically explanted full thickness human skin samples resulted an enhanced exposure of the HU177 cryptic collagen epitope primarily within the dermal region with some minor exposure detected in the epidermal regions (figure 24C). These studies suggest that while inflammatory infiltrates may contribute to and enhance the exposure of the HU177 epitope, UV-irradiation may expose the HU177 epitope within full thickness human skin in the absence of elevated levels of inflammatory infiltrates.

A.

B.

C.

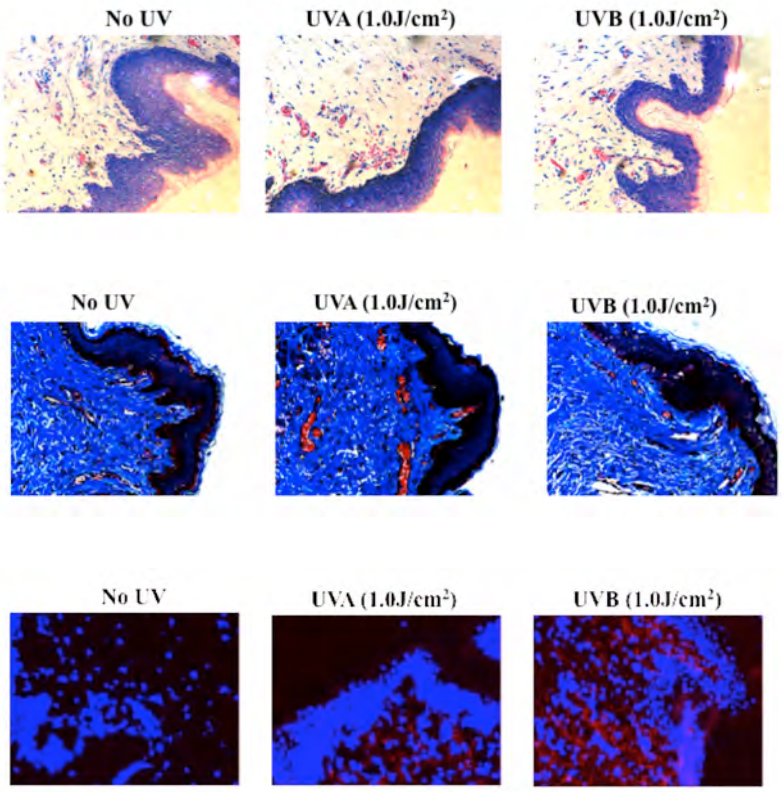

Figure 24. Detection of enhanced exposure of the HU177 epitope in ex-vivo UV-irradiated human skin. Fresh human neonatal foreskin obtained 24hrs following surgical resection was either not treated or irradiated ex vivo (1.0J/cm^2) with UVA (365nm) or UVB (310nm). Full thickness human skin was embedded and tissues sections prepared. Tissues stained by Giemsa (A), Trichrome (B) or with anti-HU177 Mab (C). A). Representative examples of human skin stained by Giemsa. B). Representative examples of human skin stained by Trichrome with blue color indicating collagen. C). Representative examples of human skin stained for exposure of the HU177 collagen epitope with Red color indicating exposure of the HU177 epitope. All photos taken at a magnification of 200x.

Figure 25. UVB-irradiation of mouse skin is associated with altered αSMA expressing fibroblast distribution. Our previous studies suggested that structural changes induced by UVB-irradiation (310nm) of collagen differentially alter human fibroblast behavior in vitro. Alpha smooth muscle actin (αSMA) is a well-known marker of activated fibroblasts and activated fibroblasts are thought to contribute to ECM remodeling during tumor development. Given our previous observations with human fibroblasts we first examined whether the human fibroblasts used in our studies expressed αSMA, a known marker of an activated phenotype. As shown in figure 25A the in vitro cultured human dermal fibroblast used in our studies indeed express αSMA confirming their activated phenotype. Given these results we next examined the relative distribution of αSMA expressing fibroblast in mouse skin before and after UV irradiation. As shown in figure 25B, irradiation of full thickness mouse skin with a single dose of UVB (0.1J/cm^2) resulted in alteration in the distribution of αSMA expressing fibroblast 24 hours later. UVB-irradiated skin exhibited enhanced levels of αSMA expressing fibroblasts within the lower regions of the dermis and appeared to be enriched around basement membrane associated structures. These data suggest that UVB may alter the distribution of αSMA expressing fibroblast that have the capacity to alter ECM structure.

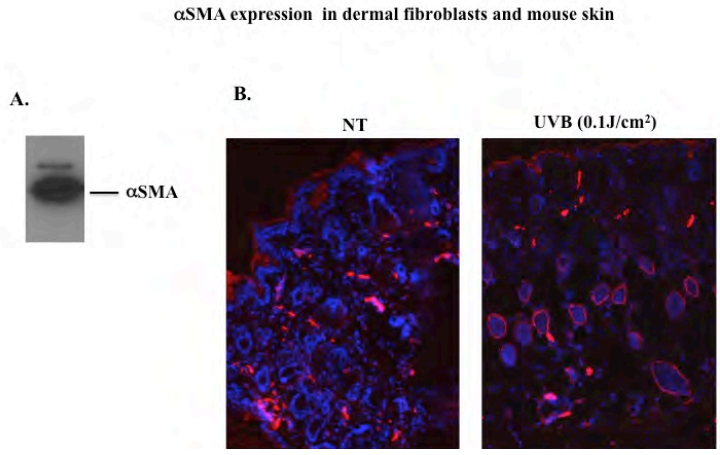

Figure 25. UVB-irradiation of mouse skin is associated with altered distribution of αSMA expressing fibroblast. A). Western blot analysis if human dermal fibroblasts for expression of αSMA. B) Murine skin from non-treated (NT) or UVB irradiated (0.1J/cm^2) animals stained for expression of αSMA (Red). Dapi stain indicated in blue.

Figure 26. Reduced migration of human dermal fibroblast following UVB-irradiation of Matrigel™. Given the differential distribution of fibroblast following UVB irradiation of full thickness skin and our previous results indicating altered adhesive behavior, we examined the impact of UVB irradiated Matrigel™ has on fibroblast migration. As shown in figure 26, a distinct reduction in dermal fibroblast migration on Matrigel™ was observed with all doses of UVB irradiation as compared to untreated Matrigel™. These data suggest that the structural changes induced within Matrigel™ by UVB irradiation reduces the capacity of dermal fibroblast to migrate under these conditions.

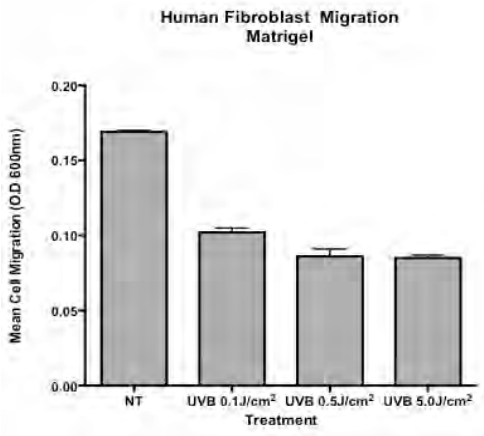

Figure 26. Reduced migration of dermal fibroblast on UVB-irradiation of Matrigel™. Matrigel™ was either non-treated (NT) or irradiated with UVB (310nm) over a dose range (0-5.0J/cm^2). Matrigel™ was coated (5.0ug/ml) on membranes from transwell inserts and blocked with BSA. Human dermal fibroblasts were seeded on the wells and allowed to migrate. Data bars represent mean cell migration (Optical Density O.D) ± standard deviations from triplicate wells.

Figure 27. UVB-irradiation of Matrigel™ enhances exposure of the HU177 cryptic epitope. Given our new data and previous observations, we examined the impact of UVB irradiation of Matrigel™ on the exposure of the HU177 epitopes using two distinct antibodies including Mab HU177 and the humanized Mab D93 directed to distinct subsets of the PGxPG containing HU177 cryptic collagen epitopes. As shown in figure 27A and B, UVB irradiation of Matrigel™ with a single dose (0.1J/cm^2) resulted in enhanced exposure of the HU177 epitopes. Importantly, irradiation of Matrigel™ in the presence of 25units/ml of the reactive oxygen species (ROS) scavenger Superoxide Dismutase (SOD) differentially reduced exposure of the HU177 epitopes. These important results suggest for the first time that the exposure of distinct subsets of the PGxPG containing HU177 cryptic collagen epitopes within the ECM preparation Matrigel™ is complex and depends in part on the generation of ROS.

A. **B.**

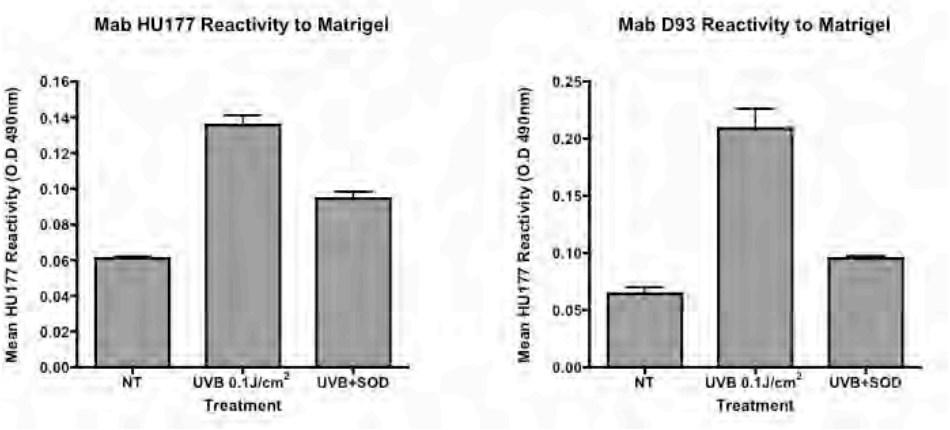

Figure 27. UVB-irradiation of Matrigel™ enhances exposure of the HU177 cryptic collagen epitope. Matrigel™ was either not treated (NT) or irradiated with UVB (310nm) at dose of 0.1J/cm^2 in the presence or absence of SOD. Wells were coated and solid phase ELISAs was carried out to assess exposure of the PGxPG containing collagen epitopes in Matrigel™. (A) Reactivity of Mab HU177. (B) Reactivity of Mab D93. Data bars represent mean reactivity of the indicated antibodies (Optical Density O.D) ± standard deviations from triplicate wells.

Figure 28. Fibroblast adhesion to Matrigel™ irradiated in the presence or absence of SOD. Our previous studies suggest a differential requirement for reactive oxygen species (ROS) for the exposure of subsets of the HU177 cryptic collagen epitope within Matrigel™. To examine whether fibroblast adhesion was altered on Matrigel™ irradiated with UVB in the presence or absence of SOD, in vitro adhesion assays were performed. As shown in figure 28, while a single dose (0.5J/cm^2) of UVB irradiation of Matrigel™ caused a small enhancement of fibroblast adhesion, this increased adhesion was decreased on UVB irradiated Matrigel™ in the presence of SOD. However, given the limited changes observed, additional experiments are required to confirm the significance of these observations. These data suggest that the generation of ROS may play a role in regulating the exposure of a cryptic site in Matrigel™.

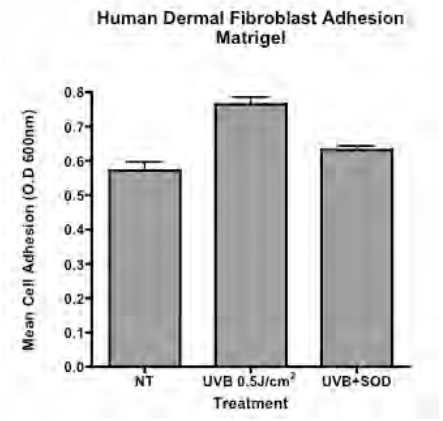

Figure 28. Fibroblast adhesion to Matrigel™ irradiated in the presence or absence of SOD. Matrigel™ was either not treated (NT) or irradiated with UVB (310nm) (0.5J/cm^2) in the presence or absence of 25units/ml of SOD. Microtiter wells were coated (5.0ug/ml) with untreated or UVB irradiated Matrigel™ and human dermal fibroblasts were seeded in wells and allowed to attach. Data bars represent mean cell adhesion (Optical Density O.D) ± standard deviations from triplicate wells.

Figure 29. Fibroblast adhesion to collagen irradiated in the presence or absence of SOD. Our previous studies suggest a differential requirement for reactive oxygen species (ROS) for the exposure of subsets of the HU177 cryptic collagen epitope within Matrigel™. To examine whether fibroblast adhesion to collagen is altered following UVB irradiation of collagen in the presence or absence of SOD, in vitro adhesion assays were performed. As shown in figure 29A, a single dose (0.5J/cm^2) of UVB irradiation of collagen type-I caused a near two-fold increase in fibroblast adhesion. Interestingly, little if any change in fibroblast adhesion to UVB irradiated collagen type-I in the presence of SOD was observed. In similar studies, while little change in fibroblast adhesion was observed between non-irradiated and UVB irradiated collagen type-IV, fibroblast adhesion to collagen type-IV irradiated in the presence of SOD was not effected (figure 29B). Taken together, these studies suggest that the generation of ROS during UVB irradiation of collagen to expose distinct cryptic sites exhibit little capacity to alter fibroblast adhesion under these experimental conditions.

A. **B.**

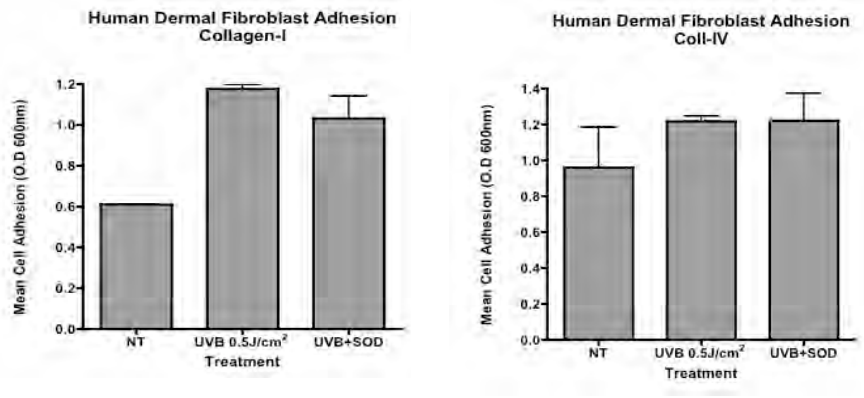

Figure 29. Fibroblast adhesion to collagen irradiated in the presence or absence of SOD. Collagen type-I (A) and collagen type-IV (B) was either not treated (NT) or irradiated with UVB (310nm) (0.5J/cm^2) in the presence or absence of 25units/ml of SOD. Microtiter wells were coated (5.0ug/ml) with untreated or UVB irradiated collagen and human dermal fibroblasts were seeded in wells and allowed to attach. Data bars represent mean cell adhesion (Optical Density O.D) ± standard deviations from triplicate wells.

Figure 30. Dose dependent enhancement of mast cell adhesion to UVB-irradiation of Matrigel™. Given previous findings suggesting the differential distribution of inflammatory cells including macrophages and neutrophils following UVB irradiation of full thickness skin and our previous results indicating altered accumulation of mast cells within UVB irradiated skin which could be inhibited by function blocking antibody D93 directed to a subset of the HU177 cryptic collagen epitopes, we examined the impact of UVB irradiated Matrigel™ has on a transformed murine mast cell line (P815). As shown in figure 30, a dose dependent increase in mast cell adhesion was observed to Matrigel™ irradiated with increasing doses of UVB. These data suggest for the first time that unique changes induced by UVB irradiation may enhances the ability of mast cells to attach to Matrigel™.

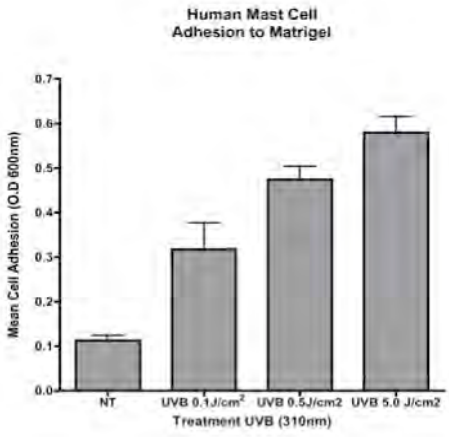

Figure 30. Dose dependent enhancement of mast cell adhesion to UVB-irradiated of Matrigel™ .Matrigel™ was either non-treated (NT) or irradiated with UVB (310) over a dose range (0-5.0J/cm^2). Matrigel™ was coated (5.0ug/ml) on microtiter wells and blocked with BSA. Murine transformed mast cells (P815) were seeded on the wells and allowed to attach. Data bars represent mean cell adhesion (Optical Density O.D) ± standard deviations from triplicate wells.

Figure 31. Reduced migration of mast cells on UVB-irradiated Matrigel™. Given the altered adhesion of mast cells to irradiated Matrigel™ and the altered accumulation of mast cells in full thickness skin following UVB irradiation, we examined the impact of UVB irradiated Matrigel™ had on mast cell migration. As shown in figure 31, surprisingly a sharp reduction in mast cell migration was observed on UVB-irradiated Matrigel™ at all doses tested as compared to untreated Matrigel™. These surprising findings suggest that the while the changes induced within Matrigel™ by UVB irradiation dose dependently enhance mast cell adhesion, these alterations have the opposite effect on mast cell migration, indicating a complex role for distinct changes in the ECM components of Matrigel™ in governing mast cell behavior in vitro.

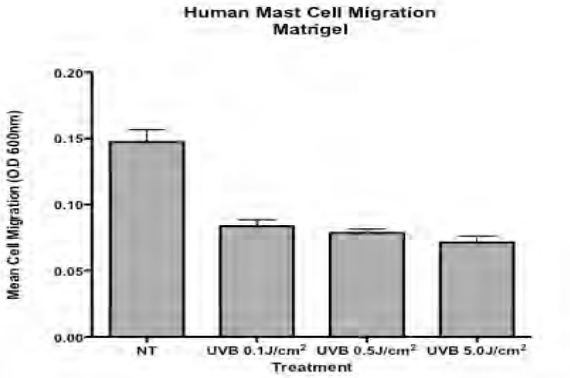

Figure 31. Reduced mast cell migration on UVB-irradiated Matrigel™. Matrigel™ was either non-treated (NT) or irradiated with UVB (310) over a dose range (0-5.0J/cm^2). Matrigel™ was coated (5.0ug/ml) on membranes from transwell inserts and blocked with BSA. Transformed murine mast cells (P815) were seeded in the upper chamber and allowed to migrate for 4hrs. Data bars represent mean cell migration (Optical Density O.D) ± standard deviations from triplicate wells.

Figure 32. Mast cell adhesion to collagen irradiated in the presence or absence of SOD. Our previous studies suggest a differential requirement for reactive oxygen species (ROS) for the exposure of a subset of the HU177 cryptic collagen epitopes within Matrigel™ and a differential impact on fibroblast adhesion to collagen. To examine whether mast cell adhesion may be altered on UVB irradiated collagen in the presence or absence of SOD, in vitro adhesion assays were performed. As shown in figure 32A, a single dose (0.5J/cm^2) of UVB irradiation of collagen type-I caused a nearly 50% increase in mast cell adhesion to collagen type-I as compared to non-irradiated collagen type-I. Interestingly, little if any change in mast cell adhesion to collagen type-I irradiated with UVB in the presence of SOD was observed. In similar studies little change in mast cell adhesion was observed between non-irradiated and UVB irradiated collagen type-IV. Moreover, mast cell adhesion to collagen type-IV irradiated in the presence of SOD was also not effected (figure 32B). Taken together, these studies suggest that the generation of ROS during UVB irradiation of collagen to expose distinct cryptic sites exhibit little capacity to alter mast cell adhesion under these experimental conditions.

A. **B.**

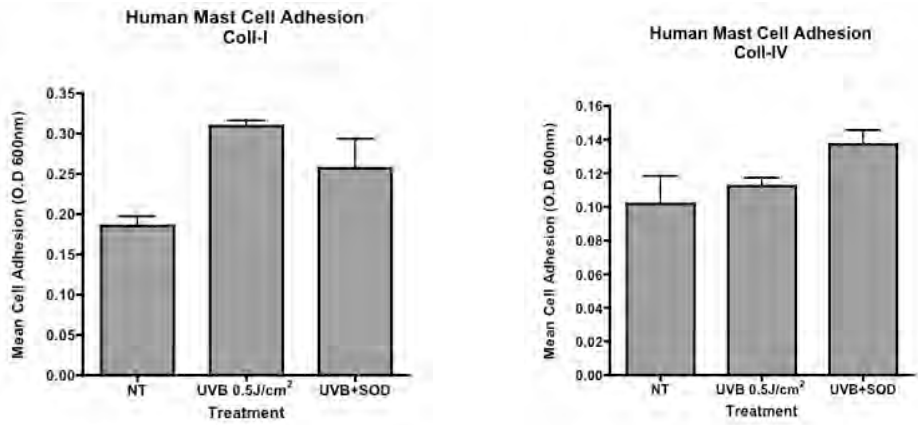

Figure 32. Mast cell adhesion to collagen irradiated in the presence or absence of SOD. Collagen type-I (A) and collagen type-IV (B) was either not treated (NT) or irradiated with UVB (310nm) (0.5J/cm^2) in the presence or absence of 25units/ml of SOD. Microtiter wells were coated (5.0ug/ml) with untreated or UVB irradiated collagen and mast cells (P815) were seeded in wells and allowed to attach. Data bars represent mean cell adhesion (Optical Density O.D) ± standard deviations from triplicate wells.

Figure 33. Detection of CD163 positive macrophages in full thickness human skin. Our previous studies have indicated that the HU177 cryptic collagen epitopes can be detected in full thickness human foreskin. To establish the experimental conditions for detecting changes in the relative accumulation of human macrophages following UV irradiation of full thickness human skin, we first examined the base line levels of human macrophages using a antibodies directed to the well –established monocyte/macrophage marker CD163. As shown in figure 33, CD163 expressing human macrophages (Red) are present at a basal level within explanted human neonatal full thickness foreskin. Importantly, macrophages can be detected in both non-irradiated as well as UVB (310nm) irradiated (0.1J/cm^2) explanted human skin. These data confirm the utility of the anti-CD163 antibody for the detection of human macrophages in frozen sections of explanted human foreskin that will be used in our human/mouse chimeric model.

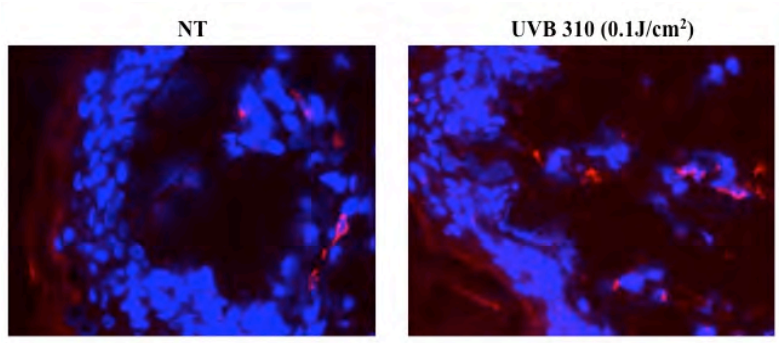

Figure 33. Detection of CD163 positive macrophages in full thickness human skin. Fresh human neonatal foreskin obtained 24hrs following surgical resection was either not treated (NT) or irradiated ex vivo (0.1J/cm^2) with UVB (310nm). Full thickness human skin was embedded and tissues sections prepared. Tissues were stained with antibodies directed to the human monocyte/macrophage marker CD163. Representative examples of human skin stained with anti-CD163 antibody. Red indicates CD163 expressing macrophages. Photos taken at a magnification of 400x.

Figure 34. Detection of αSMA expressing fibroblasts and mast cell tryptase in full thickness human skin. Our previous studies have indicated a possible redistribution of αSMA expressing fibroblasts in mouse skin following UV irradiation. In addition, an alteration in accumulation of mast cells in mouse skin was also observed. To establish the experimental conditions for detecting changes in αSMA expressing fibroblast and mast cells following UV irradiation of full thickness human skin, we examined the base line levels of αSMA (A) and mast cell tryptase (B) using antibodies directed to these well –established markers of activated fibroblasts and mast cells respectively. As shown in figure 34A, αSMA-expressing fibroblasts (Red) could be easily detected within the dermal regions of untreated or UVB-irradiated explanted full thickness human skin. In similar studies, mast cell tryptase (Red) was also readily detected within the dermal regions of untreated or UVB-irradiated explanted human skin, thereby confirming the basal levels of these markers (Figure 34B).

A. **B.**

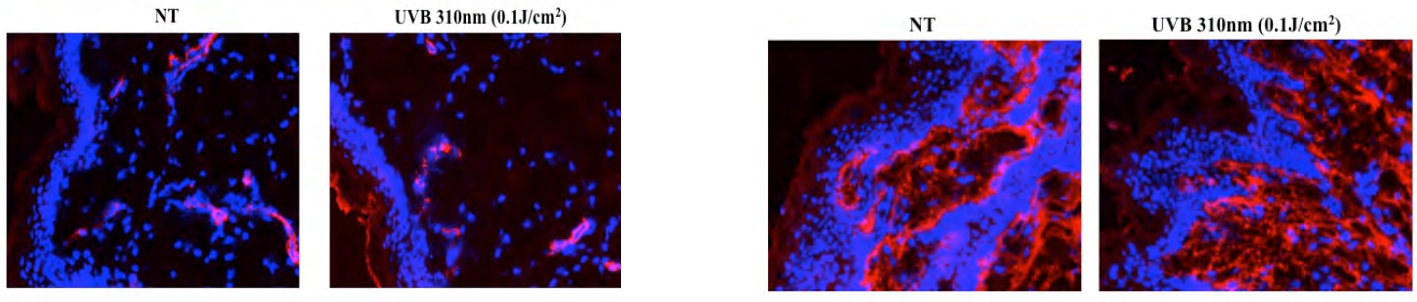

Figure 34. Detection of αSMA expressing fibroblasts and mast cell tryptase in full thickness human skin. Fresh human neonatal foreskin obtained 24hrs following surgical resection was either not treated (NT) or irradiated ex vivo (0.1J/cm^2) with UVB (310nm). Full thickness human skin was embedded and tissues sections prepared. Tissues were stained with antibodies directed to αSMA (A) and mast cell tryptase (B). Photos taken at a magnification of 200x.